European Commission

JRC TECHNICAL REPORT

Applying the Marine Modelling Framework to estimate primary production in EU marine waters

Macias, D., Friedland, R., Stips, A., Miladinova, S., Parn, O., Garcia-Gorriz, E., Melin, F.

2020

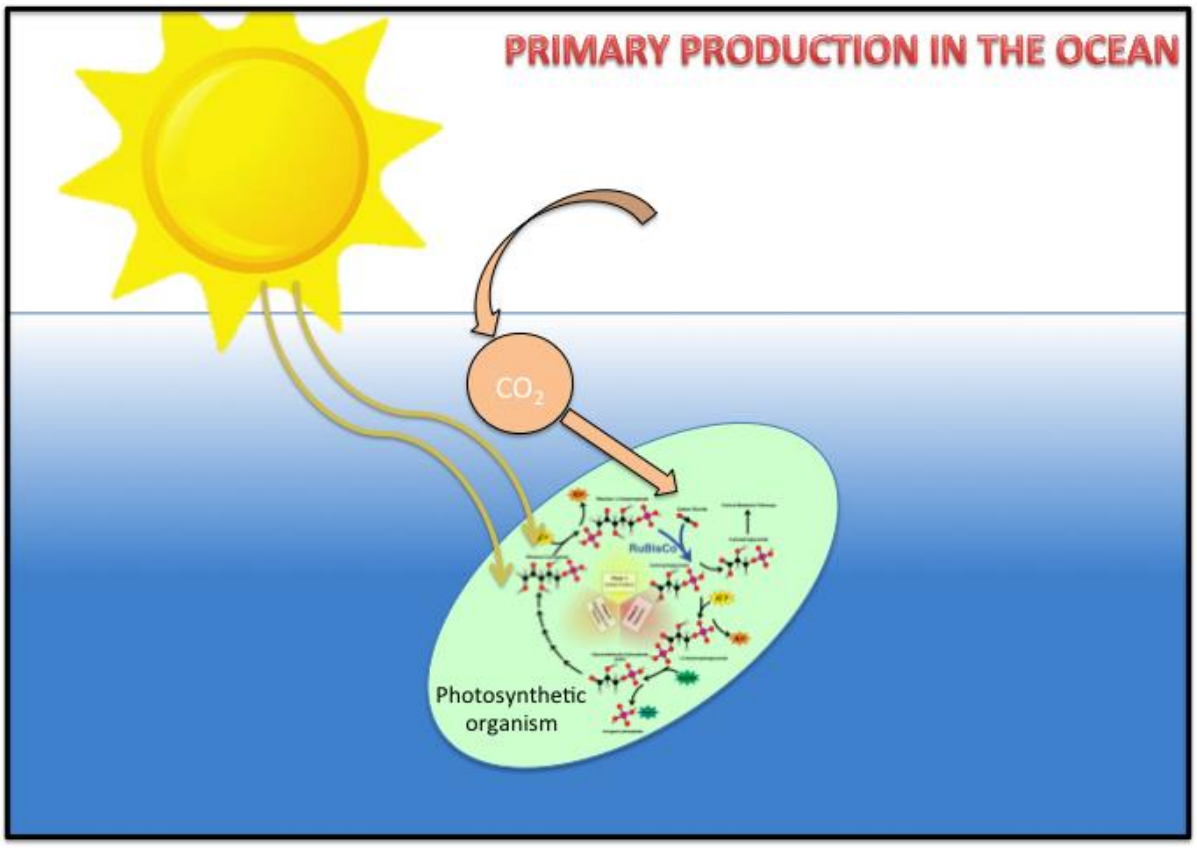

Joint Research Centre

EUR 30546 EN

This publication is a Technical report by the Joint Research Centre (JRC), the European Commission's science and knowledge service. It aims to provide evidence-based scientific support to the European policymaking process. The scientific output expressed does not imply a policy position of the European Commission. Neither the European Commission nor any person acting on behalf of the Commission is responsible for the use that might be made of this publication. For information on the methodology and quality underlying the data used in this publication for which the source is neither Eurostat nor other Commission services, users should contact the referenced source. The designations employed and the presentation of material on the maps do not imply the expression of any opinion whatsoever on the part of the European Union concerning the legal status of any country, territory, city or area or of its authorities, or concerning the delimitation of its frontiers or boundaries.

Contact information
Name: Adolf Stips
Address: Via E. Fermi, TP270, Ispra, Varese, Italy
Email: jrc-mmf@ec.europa.eu, adolf.stips@ec.europa.eu
Tel.: +39-0332-78947

EU Science Hub
https://ec.europa.eu/jrc

JRC122600

EUR 30546 EN

PDF ISBN 978-92-76-27860-3 ISSN 1831-9424 doi:10.2760/19851

Luxembourg: Publications Office of the European Union, 2020

How to cite this report: Macias, D., Friedland, R., Stips, A., Miladinova, S., Parn, O., Garcia-Gorriz, E. and Melin, F. *Applying the Marine Modelling Framework to estimate primary production in EU marine waters,* EUR 30546 EN, Publications Office of the European Union, Luxembourg, 2020, ISBN 978-92-76-27860-3, doi:10.2760/19851, JRC122600.

Contents

1 Introduction 2

2 Material and methods 5

2.1 Numerical models 5

2.1.1 Physical configuration of the different regional implementations of GETM 6

2.1.2 Biogeochemical regional models 7

2.2 Remote sensing estimates 8

2.3 Field data 10

3 Results 11

3.1 Baltic Sea 11

3.1.1 Reference values 11

3.1.2 Spatial patterns of PPR from satellite and MMF estimates 13

3.1.3 Temporal PPR analysis from satellite and MMF 15

3.1.4 Statistical comparison of PPR from satellite and MMF 15

3.2 North Sea 16

3.2.1 Reference values 17

3.2.2 Spatial patterns of PPR from satellite and MMF estimates 19

3.2.3 Temporal PPR analysis from satellite and MMF 20

3.2.4 Statistical comparison of PPR from satellite and MMF 20

3.3 Mediterranean Sea 21

3.3.1 Reference values 21

3.3.2 Spatial patterns of PPR from satellite and MMF estimates 24

3.3.3 Temporal PPR analysis from satellite and MMF 25

3.3.4 Statistical comparison of PPR from satellite and MMF 26

3.4 Black Sea 27

3.4.1 Reference values 28

3.4.2 Spatial patterns of PPR from satellite and MMF estimates 31

3.4.3 Temporal PPR analysis from satellite and MMF 32

3.4.4 Statistical comparison of PPR from satellite and MMF 34

4 Summary 35

References 37

1 Introduction

Oceans are key components of the Earth System, providing humans with valuable ecosystems services such as climate regulation, food, energy, mineral resources and cultural and recreational services. Oceans and seas are key lungs and farms of our planet, they produce half of the oxygen we breathe and 16 % of the animal protein we eat. In this sense, oceans are critical for humanity to achieve climate and societal goals within a sustainable future (Hoegh-Goldberg et al., 2019; Lubchenco and Gaines, 2019).

In the context of climate change and considering the impacts anthropogenic activities have on our planet, the oceans constitute a huge reservoir of heat that helps to maintain and regulate the Earth temperature (Abraham et al., 2013). Moreover, water-air interchange, the chemical reactions within the matrix of the seawater and the horizontal and vertical movement of water masses are all mechanisms helping to decrease the CO_2 concentration in the atmosphere, being a counter-mechanism to the greenhouse effect. This is what is typically known as the physical carbon pump (Bopp et al., 2002).

Along the same line, primary production taking place in our seas (half of the total in the planet) is another natural mechanism absorbing CO_2 from the atmosphere. This carbon is incorporated into the organic matter of marine primary producers, being phytoplankton the crucial element in this context (Duarte and Cebrián, 1996). A fraction of this carbon fixed in the organic matter is removed from the surface ocean by the sinking of particles, in a process known a biological carbon pump (Longhurst and Glen Harrison, 1989). Hence, phytoplankton does not only constitute the first trophic level in marine ecosystems being the main source of matter and energy to their food webs (Anderson et al., 2018; Richardson and Schoeman, 2004) but it also provides a very important service in helping regulate the Earth´s climate (Behrenfeld et al., 2016; Hays et al., 2005)

However, quantifying the magnitude and spatial and temporal variability of this ecosystem service is a real challenge due the difficulties for in-situ measuring. Different approaches do exist to measure primary production rates (PPR) in the ocean (and, hence, carbon uptake by phytoplankton) such as radioactive carbon uptake or oxygen production methods (Howard and Michaels, 2000). All of these methods are very time-consuming and present different limitations in terms of representativeness of the actual values in natural waters (Quay et al., 2010).

Thus, a common approach is to estimate PPR using remote sensing methods from satellites. In this case, satellites images are used to calculate the amount of chlorophyll (as a proxy for phytoplankton biomass) in the surface ocean and a theoretical model is applied to estimate the vertical distribution of the phytoplankton biomass throughout the water column. This vertical distribution is then used together with estimates of the light levels to make an approximation of the value of the integrated primary production taking place in that particular water parcel.

This approach should, thus, be able to provide synoptic maps of the magnitude of the carbon absorption into organic matter with almost global coverage and reasonable spatial and temporal resolution. Unfortunately there are a series of problems associated with these estimates: (i) surface chlorophyll estimations are not equally available or reliable for all marine regions. Factors such as cloud coverage, optical properties of the water column or even the latitude could very much affect the precision and reliability of satellite chlorophyll estimates. (ii) The theoretical models used to 'reconstruct' the vertical distribution of phytoplankton are not applicable to all marine regions. Even if

there are different algorithms and methods specifically developed for particular regions and/or seasons, it is still not possible to get accurate description of the vertical distribution of phytoplankton for many marginal sea basins (*e.g.*, Tilstone et al., 2015).

These limitations of satellite estimates are particularly relevant in many European regional seas. For example, in the ultra-oligotrophic Mediterranean Sea, standard chlorophyll estimates from remote sensing are not reliable with satellite values typically overestimating measured numbers (Uitz et al., 2012). Although the development of region-specific algorithms has decreased the bias of satellite estimates, still large deviations do exist in particular regions (e.g., the Gulf of Gabes, Adriatic coasts, etc..).

The situation is even worse in the Black Sea. The high cloudiness of this basin prevents acquiring color imagery from remote sensors during a substantial fraction of the year. This makes it almost impossible to get a reliable seasonal pattern of phytoplankton biomass in this basin from satellite data. There is also a lack of region-specific algorithms to derive chlorophyll concentration from color images with a few remarkable exceptions (e.g., D'Alimonte et al., 2012) and there is no basin-specific model to estimate the vertical distribution of plankton, probably related with the very particular hydrodynamic and chemical structure of the water masses in this region, which includes very large portions of the water column with anoxic conditions.

The problematic is quite similar in the Baltic Sea. There, the usual cloudiness together with the high latitude of this region makes standard satellite estimates of surface chlorophyll quite inaccurate. Similarly, the general models used to parameterize the vertical distribution of phytoplankton and their associated PPR typically do not provide comparable values to field data, in part also because of the particular physico-chemical characteristic of this basin (hypoxic/anoxic areas, strong pycnoclines, etc..). However, there exist already some region-specific algorithms that seem to fit better with observed data (Stramska and Zuzewicz, 2013).

For the North-Sea, the challenge for satellite PPR estimates is slightly different. This basin is relatively shallow and receives very large loads of riverine waters. This makes the color of the seawater to change and, thus, not fitted to use the standard algorithms for chlorophyll determination. Furthermore, deep chlorophyll maxima occur often during summer stratification situations (Weston et al. 2005) and it shallowness makes sediment-water interactions much more relevant than in open-ocean regions and invalidate some of the assumptions the general models for vertical distribution of phytoplankton typically contain.

Given all the specific constrains EU regional seas present to the general application of remote sensing data to estimate their primary production rate and the importance of this process for the general provisioning of services, the application of numerical models could be an adequate alternative. 3D coupled hydrodynamic-biogeochemical models can describe a number of processes occurring at the lower trophic levels of the marine webs, including the primary production rates of phytoplankton. Such numerical tools describe the cycling of limiting elements through different compartments of the food webs, typically up to zooplankton. The incorporation of nutrients, the physiological processes (mortality, remineralization, etc..) and the prey-predation interactions are all described by functional equations based on our current knowledge and understanding of those biological processes. Also the interactions between abiotic factors (such as light levels, temperature or salinity) and biological rates are routinely included in those numerical models.

However, and even if nowadays models can be highly sophisticated, they still remain a very basic description of the real ecosystems. They contain multiple simplifications and shortcuts in order to make them manageable in terms of computing needs and parameters' constrains. Hence, in order to make the models useful for decision taking, a proper comparison with available independent data is needed (i.e., model validation).

For all the reason above, the marine modeling team at unit D02 of the Joint Research Centre (JRC) has decided to perform a pan-European validation of the marine PPR estimates provided by the Marine Modelling Framework (MMF, Stips et al., 2015; Macias et al., 2018). MMF setups for four marginal EU seas (Black Sea, Mediterranean Sea, North Sea and Baltic Sea) have been used to estimate the PPR during the period 2005 – 2012, which is a good representative of common atmospheric forcings and rivers conditions (water flow and quality). Those PPR values have been compared with available independent data, both from in-situ measurement (based on literature review) and from satellite estimates in order to understand where, when and to what extent MMF computed values could be trusted and, thus, be useful for assessing this ecosystem process in EU waters. In performing those comparisons, the multiple caveats about the reliability of PPR estimates from in-situ measures and from remote sensing should be carefully considered for each individual basin.

2 Material and methods

2.1 Numerical models

The MMF developed at Unit D02 of the Joint Research Centre has been applied to simulate the hydrodynamic and biogeochemical conditions of four regional EU basins: the Baltic Sea, the North-Western European Shelf (North and Celtic Seas), the Mediterranean Sea and the Black Sea (Figure 1).

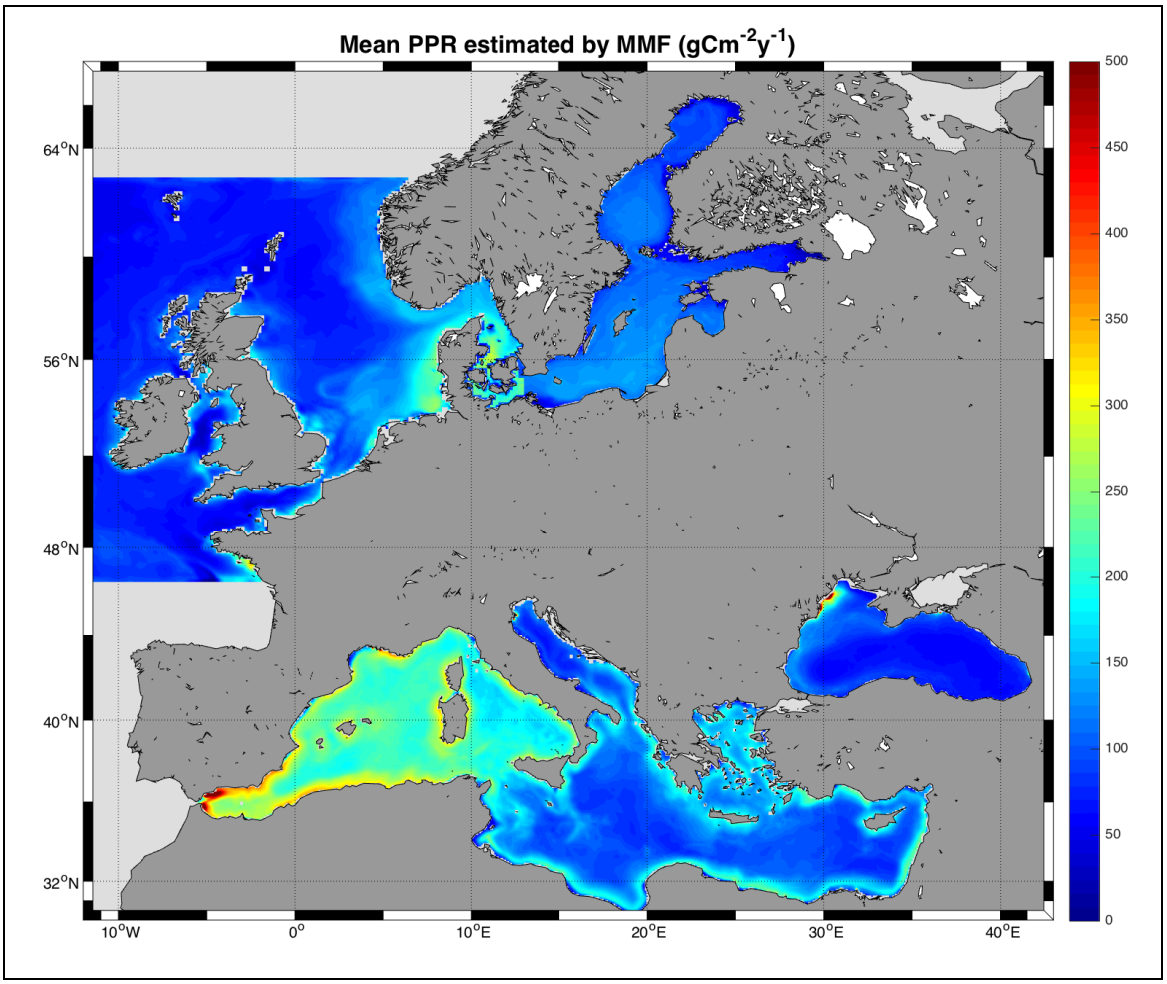

Figure 1. Mean integrated primary production rate (PPR, $gCm^{-2}y^{-1}$) computed by the MMF for the different European regional seas for the period 2005 – 2012.

The MMF is a suit of coupled models that encompasses a 'carrier' hydrodynamic module based on the general estuarine transport model (GETM, Burchard and Bolding 2002). GETM has been applied to each separate marine region individually to be able to incorporate region-specific biogeochemical models (see section 2.1.2 below).

GETM needs inputs from the atmosphere, from the land and from the open boundaries. The first two are common to all regional implementations, being ERAin atmospheric conditions from the European Centre for Medium Weather Forecast and the river conditions (water flow and quality) provided by the JRC hydrological modelling team (Grizzeti et al., in press). The boundaries for each regional model are treated differently as specified in the subsections here below.

All GETM runs covered the period 2005 -2012 for which river data is fully available although comparison with satellite estimates (see below) is performed for different subset of this period, when both datasets overlap in the different basins.

2.1.1 Physical configuration of the different regional implementations of GETM

a) Baltic Sea

The model domain covered the entire Baltic Sea area, with an open boundary in northern Kattegat. Bathymetry was interpolated to a model grid with a horizontal resolution of 2 × 2 nm. Twenty-five sigma layers were applied in the vertical (Lessin et al., 2014). The modified Winton ice model (Pärn et al., 2020) is applied. The initial distributions of water temperature and salinity were interpolated to the model grid from monthly climatological data (Janssen, 1999). The prescribed salinity and temperature distributions at the open boundary were interpolated using monthly climatological data. The atmospheric deposition of nutrients was considered constant over the entire modelling period: surface phosphate flux 0.0015 mmol P/m^2/d, nitrate flux 0.083 mmol N/m^2/d and ammonium flux 0.06 mmol N/m^2/d.

b) North Sea

The hydrodynamic setup of the North-Western European Shelf (NEWS), including the Greater North Sea as well as the Celtic Seas, has a horizontal resolution of 0.05 x 0.08 degree (~5x5.6 km; Friedland et al. 2020) and 25 vertical sigma-layers, which adapt their height dynamically to the density gradient (Gräwe et al., 2015). The bathymetry is taken from North-West European Shelf Operational Oceanographic System (NOOS), but adjusted along some shallow parts of the Wadden Sea. Initial conditions were obtained from a long-term model run (Friedland et al., 2020). Along the open boundaries in the Atlantic Ocean, salinity and water temperature were prescribed using monthly climatological vertically-explicit values, computed from the World Ocean Database. Sea level data and surface currents at the open boundaries were generated in temporal resolution of 30 minutes from the tide model provided by Oregon State University (http://volkov.oce.orst.edu/tides/AO.html) and enhanced by the daily deviation from the long-term mean using HYCOM (Cummings and Smedstad, 2013).

c) Mediterranean Sea

GETM set-up for the Mediterranean has a horizontal resolution of 5′ x 5′ (~9x9km) and includes 25 vertical sigma-layers. Model bathymetry was built using ETOPO1 (http://www.ngdc.noaa.gov/mgg/global/) database while initial and boundary thermohaline conditions were created by using the Mediterranean Data Archeology and Rescue-MEDAR/MEDATLAS database (http://www.ifremer.fr/medar/). The salinity, temperature and biogeochemical variables used as initial conditions at the start of the model integration (i.e., 2005) were obtained from a long-term model run starting in 1989 and described in Macias et al., 2019.

Boundary conditions at the western entrance of the Strait of Gibraltar were computed from the Mediterranean Data Archeology and Rescue-MEDAR/MEDATLAS database (http://www.ifremer.fr/medar/) imposing monthly climatological vertically-explicit values of salinity. No horizontal currents were imposed at the open boundary. With this boundary configuration the circulation through the Strait is established by the internally-adjusted baroclinic balance provoked mainly by evaporation and deep-water formation within the basin (Macias et al., 2016).

d) Black Sea

The Black Sea hydrodynamic model comprises of GETM, http://www.getm.eu/) and GOTM initialized on high-resolution 2 x 2 min latitude–longitude horizontal grid. The model bathymetry grid is produced from ETOPO1 with horizontal resolution of 1 min. The maximum depth of the model domain is 2200 m with a 70 levels general vertical grid, which is compressed towards the surface. This model has been successfully applied to simulate the long-term evolution of the Black Sea thermohaline structure and circulation (Miladinova et al., 2017). The model is initialized by means of temperature and salinity 3D fields coming from the MEDAR/MEDATLAS II project (http://www.ifremer.fr/medar).

2.1.2 Biogeochemical regional models

All biogeochemical models described below are online coupled to GETM through the Framework for Aquatic Biogeochemical Models (FABM, https://sourceforge.net/projects/fabm/, Brueggeman and Bolding 2014).

These biogeochemical models are based on deterministic descriptions of the processes involving the dynamic of the low-trophic levels of the marine ecosystems, from nutrients to zooplankton. Basically, they allow simulating the incorporation of nutrients by phytoplankton, the assimilation of those inorganic components into the organic matter and the transference of this matter within the food web, both by zooplankton grazing and by recycling via the microbial loop.

Each adopted model has a different level of complexity in the description of the low trophic food web as requested by the essentially different characteristics of the diverse marine ecosystems.

a) Baltic Sea

The MSI-ERGOM model version applied in this study included three functional groups of phytoplankton—diatoms, dinoflagellates, and cyanobacteria; bulk zooplankton group; nitrate, ammonium, and phosphate nutrients; dissolved oxygen; pelagic and benthic detritus; and iron-bound phosphorus in water. The corresponding set-up was previously developed and used by Lessin et al. (2014). Typical initial concentrations of biogeochemical variables were prescribed uniformly within the model domain.

b) North Sea

The freely available ERSEM (https://gitlab.ecosystem-modelling.pml.ac.uk/stable/ERSEM) was used as biogeochemical model for the NWES setup. ERSEM consists of dissolved inorganic nutrients and has a sophisticated growth model for four functional phytoplankton groups, which have specific ecological requirements. Nutrient uptake is assumed in a variable C:N:P ratio , what allows the single phytoplankton groups to adapt their growth to changes of the nutrient limitations. Previous studies

(Butenschoen et al., 2016; Ford et al., 2017) have shown a good agreement of the different modelled phytoplankton groups with observations. For the present study, the benthic model with the lowest complexity, the so-called 'benthic returns', was used to reduce the computational efforts.

c) Mediterranean Sea

For the Mediterranean Sea, the biogeochemical code is named MedERGOM (Macias et al. 2014a and 2014b). MedERGOM is a modified version of the ERGOM model (Neumann, 2000) specifically adapted to represent the conditions of the pelagic ecosystem of the Mediterranean Sea. It has proven useful to describe present (Macias et al. 2014b), past (Macias et al. 2014a) and future (Macias et al. 2015) biogeochemical conditions in this semi-enclosed basin. The latest version of this code (the one used in the present work) has been also modified to account for flexibility in the relative nutrient incorporation ratio according to the 'line of frugality' concept (Galbraith and Martiny, 2015; Macias et al., 2019).

d) Black Sea

The evolution of the low trophic level components of the food chain in the Black Sea ecosystem is simulated by BSEM (Black Sea Ecosystem Model) (Miladinova et al., 2020). BSEM is a nitrate-based biogeochemical model based on the existing models (Oguz et al., 1999, 2000, 2014). The model is purposefully adapted for the Black Sea basin, where a unique ecosystem exists. It represents the classical omnivorous food-web with 12 state variables.

2.2 Remote sensing estimates

The quasi-synoptic view provided by remote sensing images has been used to try to obtain comprehensive and large-scale information about the status of marine ecosystems. Color images could be used to estimate the surface distribution and concentration of phytoplankton biomass by relating the leaving radiance with chlorophyll concentration in the surface layer of the ocean (Behrenfeld and Falkowski, 1997). Using this information and estimates of the sea surface temperature and of the vertical light profile, it is possible to approach the PPR taking place in the water column by applying different vertical algorithms (models).

One of the most commonly used methods is the Vertically Generalized Production Model (VGPM) developed by Behrenfeld and Falkowski (1997). It uses estimates of surface chlorophyll, SST, PAR, euphotic depth and the optimum photosynthetic rate of phytoplankton (P^b_{opt}) to calculate the integrated PPR in the euphotic layer of the ocean. The calculations done by this method depends largely on the relationship between SST and P^b_{opt} which is empirically determined by a seventh-order polynomial function. VGPM works well to open-sea, relatively oligotrophic regions so it has been used to compute satellite estimates of PPR for the Mediterranean Sea, although standard chlorophyll products are usually overestimating actual values in the low range of concentrations for this basin (e.g., Volpe et al. 2007). Unfortunately it is not suitable to represent the conditions of the other EU regional seas (e.g., Campbell et al., 2002; Stramska and Zuzewick, 2013).

Another estimate of primary production from remote sensing data is based on a depth-resolved and wavelength-resolved model (Mélin and Hoepffner 2011) following the original formalism described by Platt and Sathyendranath (1988) and implemented at global scale by Longhurst et al. (1995).

At any given location and time, the model considers the total irradiance available for photosynthesis between 400 and 750 nm, the phytoplankton biomass indexed by the concentration of chlorophyll-a obtained by remote sensing, as well as the physiological capacity of phytoplankton organisms to perform photosynthesis. The spatial and temporal changes in phytoplankton metabolism and its vertical distribution are considered in the model through the partition of the global ocean into biomes and provinces within each of which the photosynthesis – irradiance parameters and the shape of the depth profile of chlorophyll are assigned according to knowledge acquired from field observations. Direct and diffuse spectral light is derived from total PAR (Mélin et al. 2004) and is transmitted through the water surface and then propagated till extinction (to the 0.1% light level) or the bottom. In this propagation, light is absorbed and scattered by pure sea-water, phytoplankton, non-pigmented particles and chromophoric dissolved organic matter (all indexed as a function of chlorophyll). Part of the light absorbed by phytoplankton is used for photosynthesis through the use of photosynthesis-light curves defined regionally (Mélin and Hoepffner 2004) and represented by 2 parameters, the initial slope of the photosynthesis-light curve, commonly designated by alpha (α^B), which represents the photosynthetic response of phytoplankton chlorophyll to an increase in irradiance; and the assimilation number, commonly designated as P^B_{max}, which refers to the maximum photosynthetic rate of phytoplankton chlorophyll under saturating light for the prevailing environmental conditions. These calculations are performed at regular intervals during the day to account for changes in illumination geometry. The final result is the daily depth-integrated areal primary production. The inputs are standard SeaWiFS chlorophyll and PAR monthly products at a resolution of $1/12^{th}$ degree. Even though the model setting is global, it is stressed that the photosynthetic parameters and the shape of the vertical chlorophyll profile vary regionally.

In validation exercises (comparison with field measurements of primary production), the model compared favorably with respect to other models (Carr et al. 2006, Friedrichs et al. 2009, Saba et al 2010, 2011). However, it is acknowledged that the model outputs suffer from higher uncertainties in coastal regions, a primary reason for this being the uncertainties associated with standard satellite data of chlorophyll and the difficulty in representing the light field in the water column in optically complex waters. To partly alleviate this issue, a specific version of the model (Mélin & Vantrepotte 2007) has been used in the Black Sea. In that case, in-water products of absorption and backscattering are derived using the Quasi-Analytical Algorithm (QAA, Lee et al. 2002) that should be more efficient across various types of water. The chlorophyll concentration is related to phytoplankton absorption through an empirical formula (Bricaud et al. 1995). The propagation of the light field through the water column should also be improved by considering the independent effects of the absorption by phytoplankton, dissolved organic matter and non-pigmented particles and the scattering by particles. As for the global setting presented above, the photosynthetic

parameters and the shape of the vertical chlorophyll profile are specific to the Black Sea. With respect to the global calculations, the spatial resolution is 2-km.

2.3 Field data

As commented above, in situ measurement of PPR is cumbersome, slow and not particularly accurate. Typically, water samples have to be taken into closed containers and incubated under different lights conditions and with radioactive ^{14}C. The incorporation rate of this carbon isotope is estimated in laboratory conditions and from that rate a primary production rate is calculated for each sampled depth. Those individual data are then fitted to a light-growth curve, the fitting coefficients of this curve are used to estimate the integrated primary production rate of the water column in that particular position of the sea. So, even the 'in-situ' PPR data is only an estimate, depending on the quality of the sampling, the accuracy of the laboratory measures and the representativeness of the light-growth curve for the real phytoplanktonic behavior in the water column.

Given those constrains, it is impossible to obtain synoptic, large-scale information on PPR from field measurements. However, we have gathered as much data as possible from published works in the different basins in order to assess both the MMF and the satellite estimates. For each basin, the collected field measurements are presented in the corresponding tables shown below.

3 Results

For each regional sea there is an specific subsection containing the following information:

- A brief description of the hydrodynamic and biogeochemistry characteristics of the basin
- A compilation of observed/measured PPR values (including references) and the mean values of the estimates from satellite and the MMF
- A set of spatially-explicit maps with the mean distributions of PPR from satellite and MMF computed for the common time-period in both datasets (basin-specific)
- Analysis of the seasonal cycle of PPR from satellite and MMF
- Statistical analysis of the spatial and temporal dynamics of PPR from both sources

3.1 Baltic Sea

The Baltic Sea is a semi-enclosed sea, surrounded by heavily populated countries and, hence, subjected to heavy anthropogenic impacts. Among others, eutrophication induced by (mainly) riverine nutrient inputs is a very important ecosystem stressor in the basin, causing harmful algal blooms and anoxic conditions in several regions. Measures to fight against human-induced eutrophication in this regional sea have been implemented since decades, e.g. within the Baltic Sea Action Plan (2007, 2013) but their effects on ecosystem status are (at best) moderate (Andersen et al., 2017). Hence, it is fundamental to develop and apply tools than can help link the land-based measures to reduce alloctonous nutrients inputs with changes in the status of marine ecosystems.

Numerical models such as the MMF can serve this purpose, especially due to the difficulties to estimate the different ecosystem variables from remote sensing (*e.g.*, Stramska and Zuzewick, 2013), because of (i) the high latitude of this basin (that reduces the frequency of satellite coverage), (ii) its typical high cloudiness, (iii) the large land-sea interferences along the coasts and (iv) the high amount of organic material (e.g. CDOM). Satellite-derived PPR estimates come from a global distribution where phytoplankton photosynthetic parameters and vertical profiles are adapted for the Baltic Sea; however, input chlorophyll data are obtained with standard global algorithms and the in-water bio-optical algorithm is developed for open oceans, assumptions not appropriate for the Baltic Sea in most conditions.

3.1.1 Reference values

Table 1 shows a compilation of PPR values from different sources for the Baltic Sea; in-situ, satellite and model. Measured mean and standard deviation values could not be directly compared with satellite and MMF estimates, as the spatial and temporal coverage of those datasets are not coincident. However, this comparison allows assessing how far apart the different datasets are, and if estimated values fall within the observed range in situ.

Area	PPR (gC m^{-2} y^{-1}) ^{14}C method	PPR (gC m^{-2} y^{-1}) MMF	PPR (gC m^{-2} y^{-1}) Satellite	Reference for the ^{14}C values
Baltic Sea	165	115 (25)	395	Wasmund et al., 2001
Gulf of Gdansk	190	122	436	Renk, 1993
Gdansk deep	173	135	364	
Gotland Sea	141	116	365	
SE Baltic	255	140	367	Wasmund et al., 2001
Gulf of Riga	353 – 376	190	494	Purina et al., 2018
Gulf of Riga	250			Andrushaitis et al., 1992
Gulf of Riga	350			Oelsen et al., 1999
MEAN (RANGE)	**234(144 - 324)**	**136(121 - 151)**	**403(351 - 455)**	

Table 1. Compilation of PPR values from different sources for diverse regions in the Baltic Sea

Mean measured PPR values in the Baltic Sea are higher than MMF estimates as much of the reported numbers have been measured in very productive, coastal settings (such as the Gulf of Riga of the Gulf of Gdansk). In such coastal and shallow regions, model estimates are lower than measured values. However, for the open sea regions and for the average value of PPR in the entire basin, MMF and measures seems to agree quite reasonably. In fact, integrated estimates of the PPR for the entire Baltic Sea from field data measurement range between $62*10^9$ and $49*10^6$ tC y^{-1} (Wasmund et al., 2001), while the MMF provide a mean annual integrated PPR of $42*10^6$ tC y^{-1} not far from previous numbers.

Satellite estimates, on the contrary, are much higher than both measures and MMF estimations. In fact, there is a factor of almost 2 overestimation with respect to field data and a factor 4 with respect to modeled values. As commented above, this particular region is challenging for satellite estimates so actual numbers could not be fully trusted in this basin.

The scatter plot of measured vs. estimated PPR values (Fig. 2) clearly shows the sub-estimation by MMF and the over-estimation by satellite. In both cases, however, there is a reasonable correlation between the different datasets while the absolute bias is lower for the case of the MMF (73 $gCm^{-2}y^{-1}$) than for satellite estimates (194 $gCm^{-2}y^{-1}$).

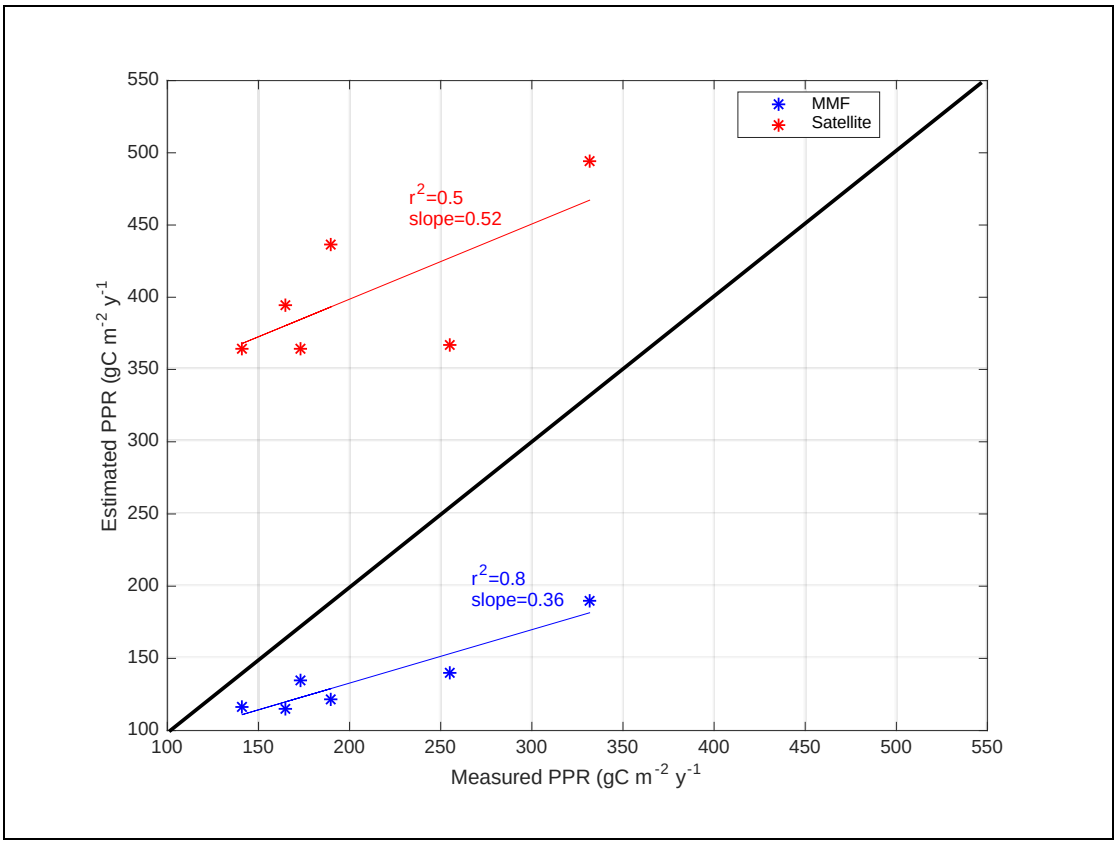

Figure 2. Measured PPR versus estimated PPR for the different regions in the Baltic Sea as shown in Table 1. The thick black line indicate the 1:1

Hence, mean values computed by MMF are somewhat lower than reported figures although they are located approximately on the same range.

3.1.2 Spatial patterns of PPR from satellite and MMF estimates

As commented above, for this basin exact values from satellite estimates should not be trusted as they overestimate quite largely the scattered field measurements reported in the literature. In any case, it could be useful to compare the spatial patterns from the satellite and the model maps during their common overlapping period (2005 to 2007).

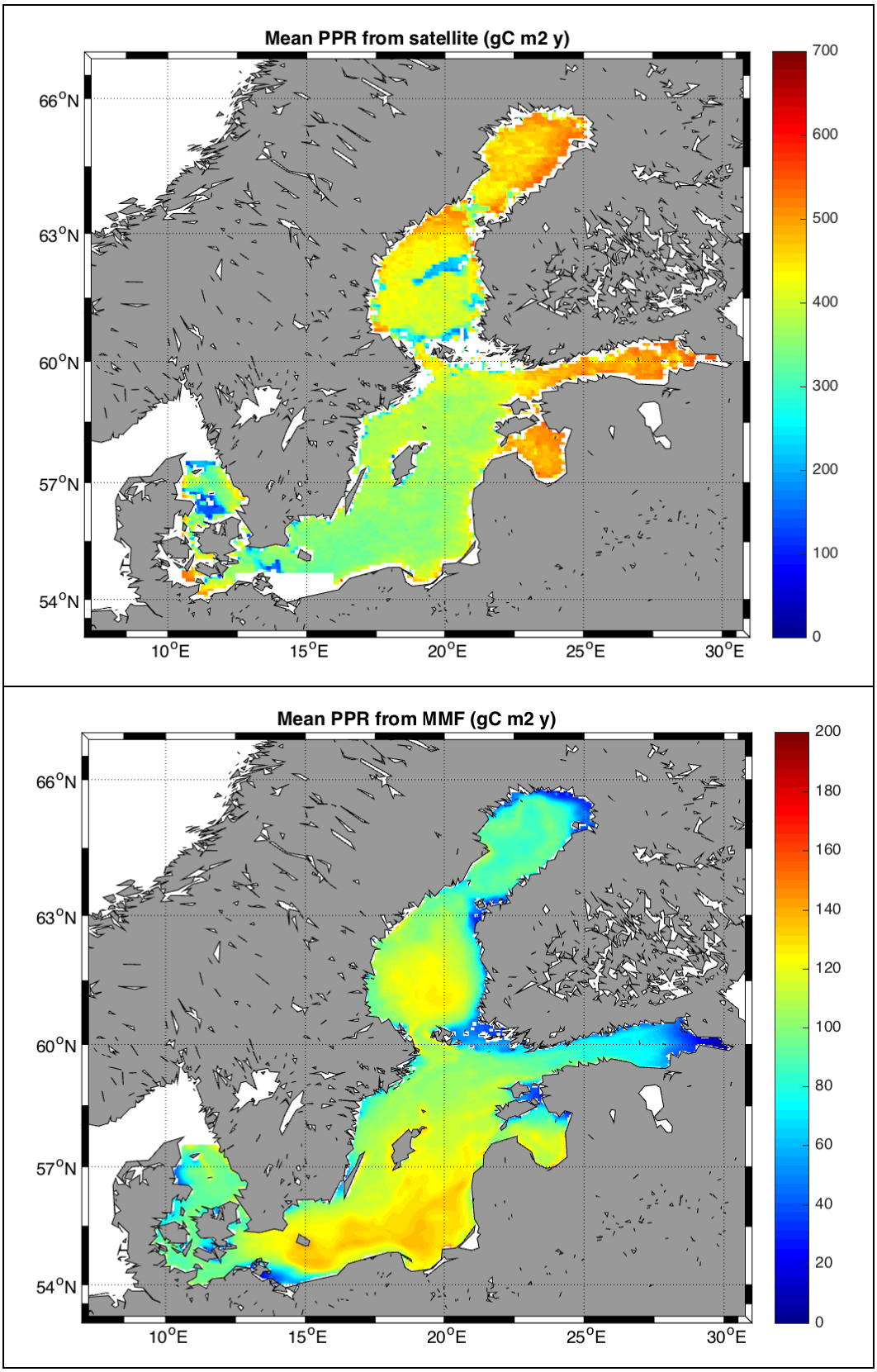

Figure 3. Baltic Sea PPR estimates. Upper panel, mean PPR estimated by remote sensing for the period 2005 – 2007. Lower panel, mean PPR estimated by the MMF for the period 2005 – 2007.

There are similitudes and differences in the spatial distribution of PPR estimated from remote sensing and from MMF (Fig. 3). In MMF maximum PPR levels are simulated in the south-east corner of the basin and within the Bothnian Sea while maximum satellite estimates are located in the Gulf of Finland and towards the northernmost region of the Baltic. The Gulf of Riga appears as a quite productive area in both estimates while the Danish Straits show intermediated PPR values.

3.1.3 Temporal PPR analysis from satellite and MMF

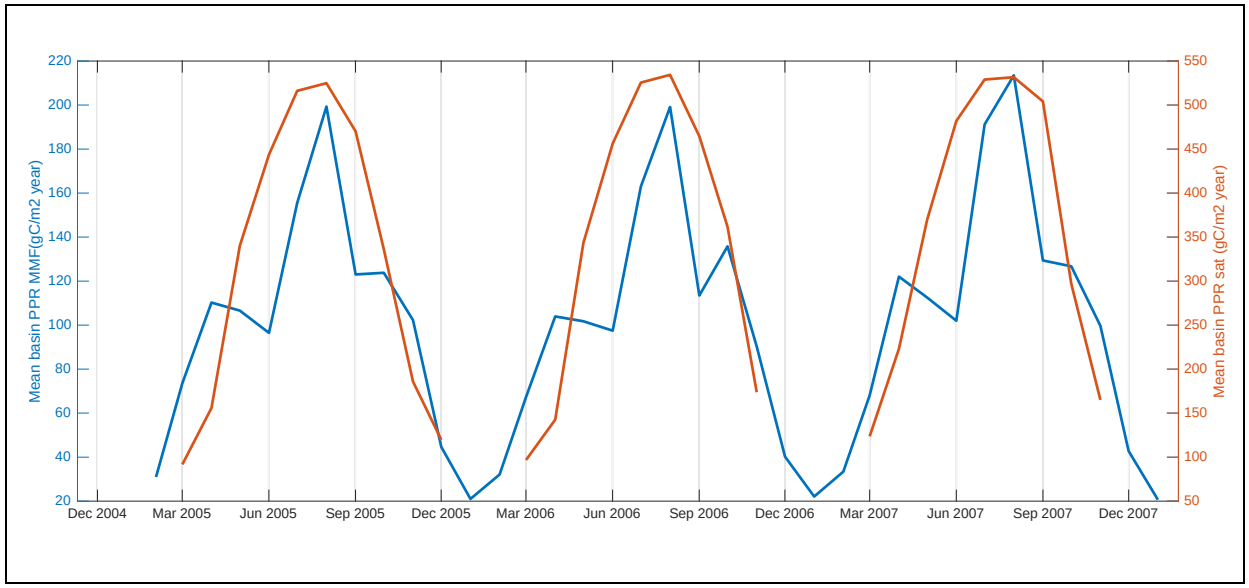

Figure 4. Baltic Sea mean, basin-wide PPR monthly values from MMF and satellite during the 2005 – 2007 period.

Figure 4 shows that, even if absolute numbers can´t be compared (notice the different y-scales) the temporal dynamics of basin-wide integrated PPR is actually quite similar in MMF and in remote sensing datasets. The maximum PPR levels are recorded towards the end of summer (August) while minimum values are coincident with the winter (December – January). It is also worth mentioning that in none of the studied years there is satellite information for the winter months in relation to cloud coverage and low solar elevation.

3.1.4 Statistical comparison of PPR from satellite and MMF

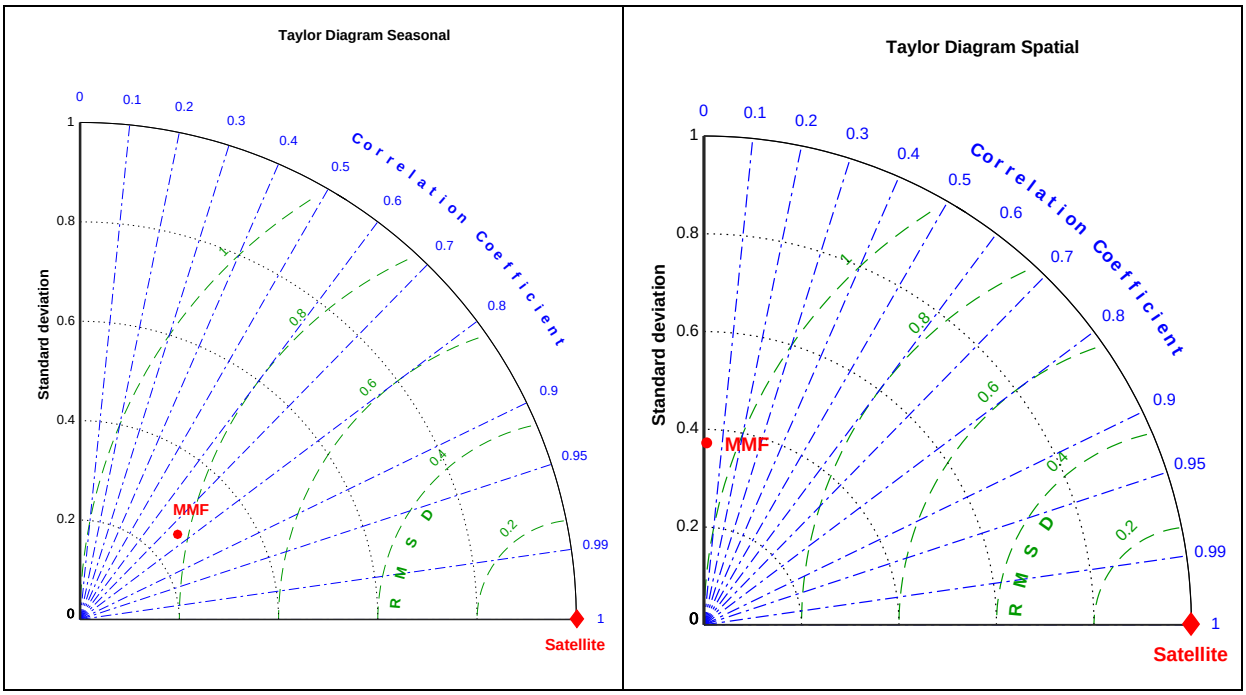

Figure 5. Left panel, Taylor Diagram of the monthly values comparison (shown in Fig. 4). Right panel, Taylor Diagram of the spatial distributions comparison (Fig. 3).

The Taylor Diagrams shown in Fig. 5 clearly indicate that even if the seasonal dynamics is quite similar in both MMF and satellite estimates (r^2=0.78), there is a very large bias as shown by the large value of the RMSD. Contrary, the spatial distribution is very different in both MMF and satellite (Fig. 5, right panel) with very low correlation coefficient and a very large value of the RMSD.

3.2 North Sea

The North Sea is a very productive marine region receiving high amounts of nutrient inputs from various sources such as riverine and atmospheric inputs. Even if the North Sea is one of the most studied marine regions of the world, there is still a lack of understanding on how much anthropogenic-derived inputs are shaping and influencing primary production and eutrophication levels in this marginal sea.

In order to investigate this connection, it is necessary to quantify the primary production in the basin, along with its variability in space and time. However, remote sensing provides very fractional and inaccurate estimates for this shallow region due to its cloudiness, the presence of subsurface chlorophyll maxima (e.g., Weston et al., 2005, Hickman et al. 2012) and the particular optical characteristics of its seawater shaped by high concentrations of suspended material (e.g. SPM). Hence, there is a high demand to develop numerical models that can accurately reproduce the PPR characteristics in this marine region.

3.2.1 Reference values

As done in the previous section, table 2 shows individual measured values of integrated PPR in the North Sea (from the literature) along with the mean and standard deviation of the estimates from satellite and MMF for the period 2005 – 2007 (their common overlapping period). The same caveats as above apply to this comparison regarding the representativeness of mean values from the different datasets. This is not a straight, one-to-one validation but serves to understand how far apart the two estimates are from the range of measured values.

Area	PPR (gC m^{-2} y^{-1}) 14C	PPR (gC m^{-2} y^{-1}) MMF	PPR (gC m^{-2} y^{-1}) Satellite	Reference for the ^{14}C values
North Sea	150 - 250	116 (47)	341(107)	Anon, 1993
North Sea	79 - 261			Join & Pomroy, 1993
Northern N.S.	54 - 127	89 (28)	278(85)	Steele, 1956
Southern N.S.	200 - 250	136 (41)	411(94)	Fransz & Gieskes, 1984
Continental coast (S. N.S.)	200 (250)			Emeis et al. (2015)
Belgium coast	320	240 (44)	489(60)	Joiris et al., 1982
Central N.S.	265 (168 – 372)	95 (28)	301(74)	Weston et al., 2005
ICES Box 3 (east coast of UK)	79	114	430	Joint & Pomroy, 1993
ICES Box 4 (Belgium coast/ S.N.S.)	199	130	439	
ICES Box 5 (German Bight/ S.N.S.)	261	180	477	

ICES Box 7 (southern part of Central N.S.)	119	90	283	
MEAN (RANGE)	**200 (102 - 298)**	**135 (74 - 196)**	**364 (278 - 450)**	

Table 2. Compilation of PPR values from different sources for the North Sea.

Mean values from the three different datasets in the North Sea are similar to those for the Baltic Sea still indicating a mesotrophic sea region (*e.g.*, Skogen and Moll, 2001). There are, however, strong gradients in the spatial distribution of PPR in this region (see section b) below), also showing strong seasonality (see section c) below). That makes the comparison of mean or integrated values more complicated.

The scatter plot of measured vs. estimated PPR values (Fig. 6) clearly shows the sub-estimation by MMF and the over-estimation by satellite as reported for the Baltic Sea in the previous section. In both cases, however, there is a reasonable correlation within the different datasets while the absolute bias is lower for the case of the MMF (82 $gCm^{-2}y^{-1}$) than for satellite estimates (147 $gCm^{-2}y^{-1}$).

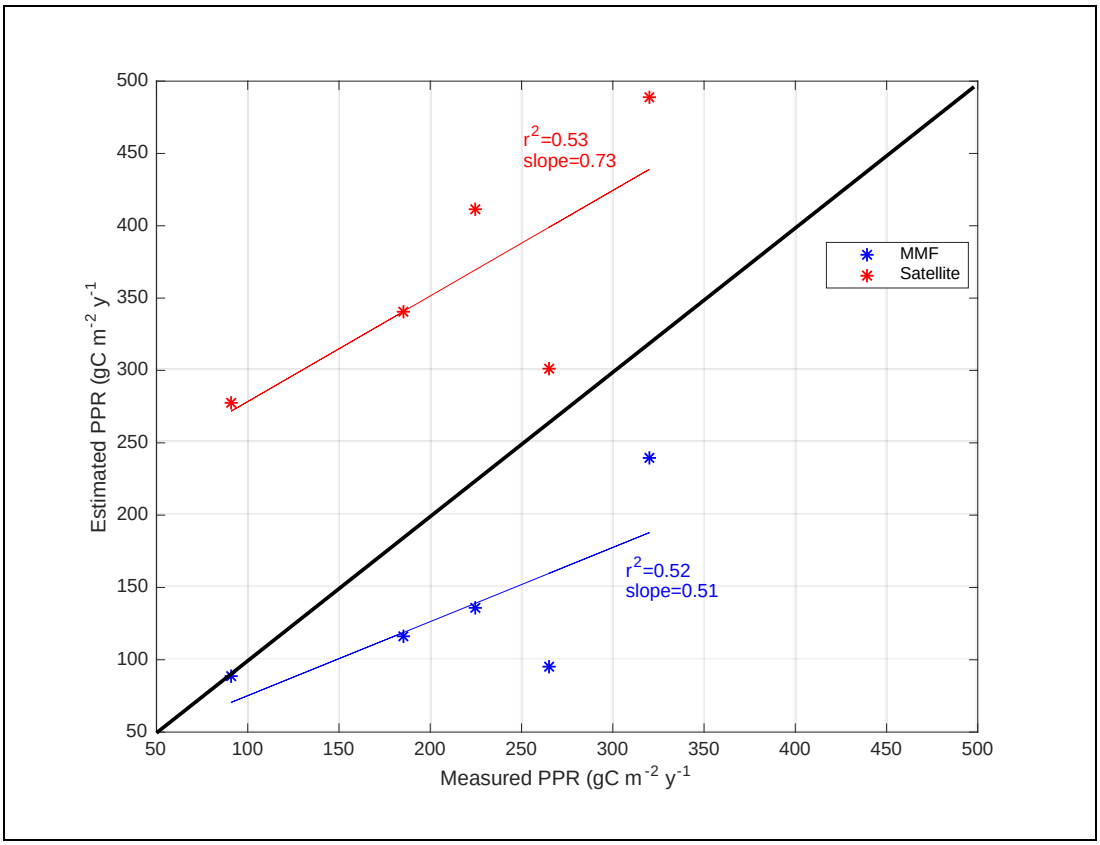

Fig. 6. Measured PPR versus estimated PPR for the different regions in the North Sea as shown in Table 2. The thick black line indicate the 1:1

In spite of the differences shown above, the range of measured PPR values and estimations are similar, indicating that the MMF and satellite dataset used here could be considered a reasonable representation of actual values in this particular region of the ocean.

3.2.2 Spatial patterns of PPR from satellite and MMF estimates

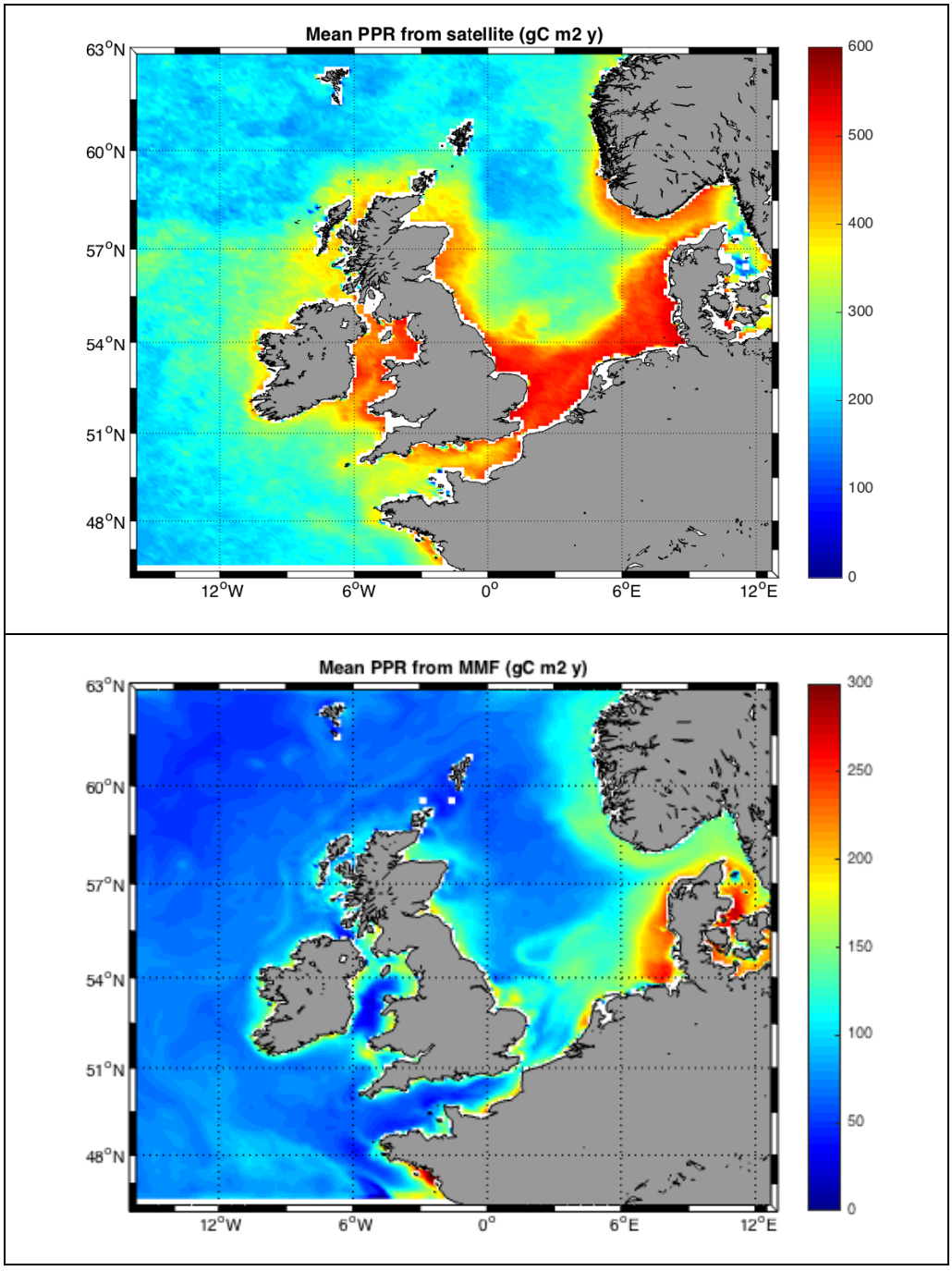

Figure 7. NWES Sea PPR estimates. Upper panel, mean PPR estimated by remote sensing for the period 2005 – 2007. Lower panel, mean PPR estimated by the MMF for the period 2005 – 2007.

Even if the absolute PPR values are quite different in satellite and MMF estimates (Fig. 7, note the different colorbars), their spatial distributions are quite similar. Higher PPR are estimated for the coastal regions, particularly in the southern shores of the North Sea, a progressive diminution of PPR is estimated by both datasets towards the open sea regions.

3.2.3 Temporal PPR analysis from satellite and MMF

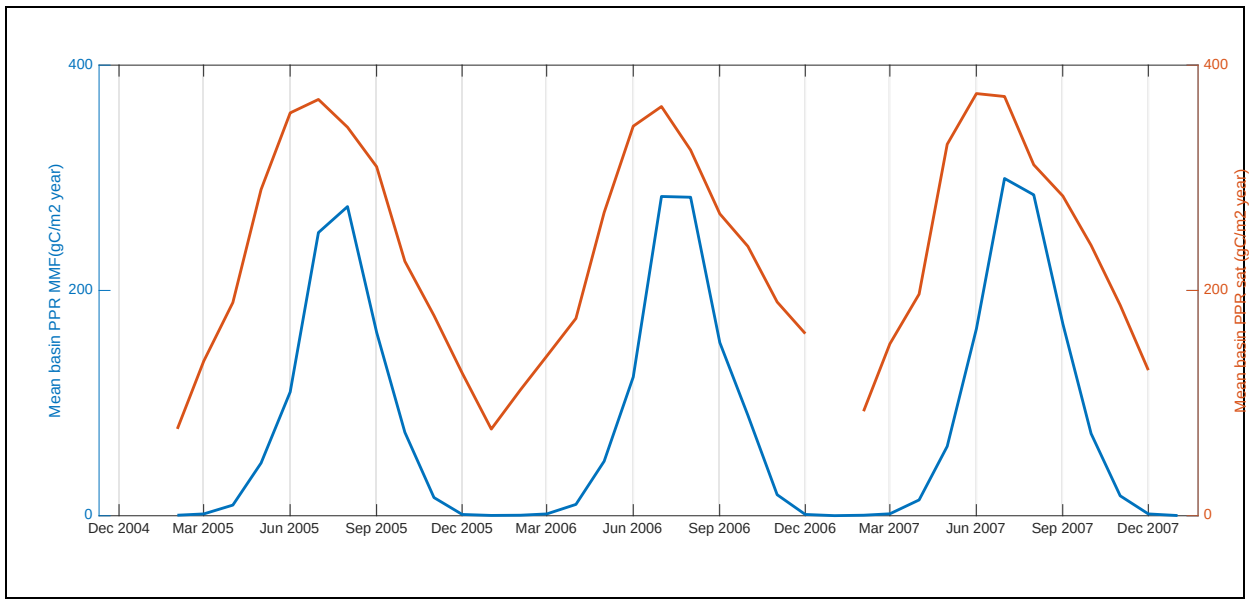

Figure 8. NW Sea mean, basin-wide PPR monthly values from MMF and satellite during the 2005 – 2007 period.

Figure 8 shows that the temporal dynamics of basin-wide integrated PPR is actually quite similar in MMF and in remote sensing datasets. The maximum PPR levels are recorded towards the end of summer (July - August) while minimum values are coincident with the winter (December – January). This figure also shows that differences between MMF and satellite estimates are larger during the low-productivity period in winter, when MMF estimates a very low PPR value while satellite reports much higher values.

3.2.4 Statistical comparison of PPR from satellite and MMF

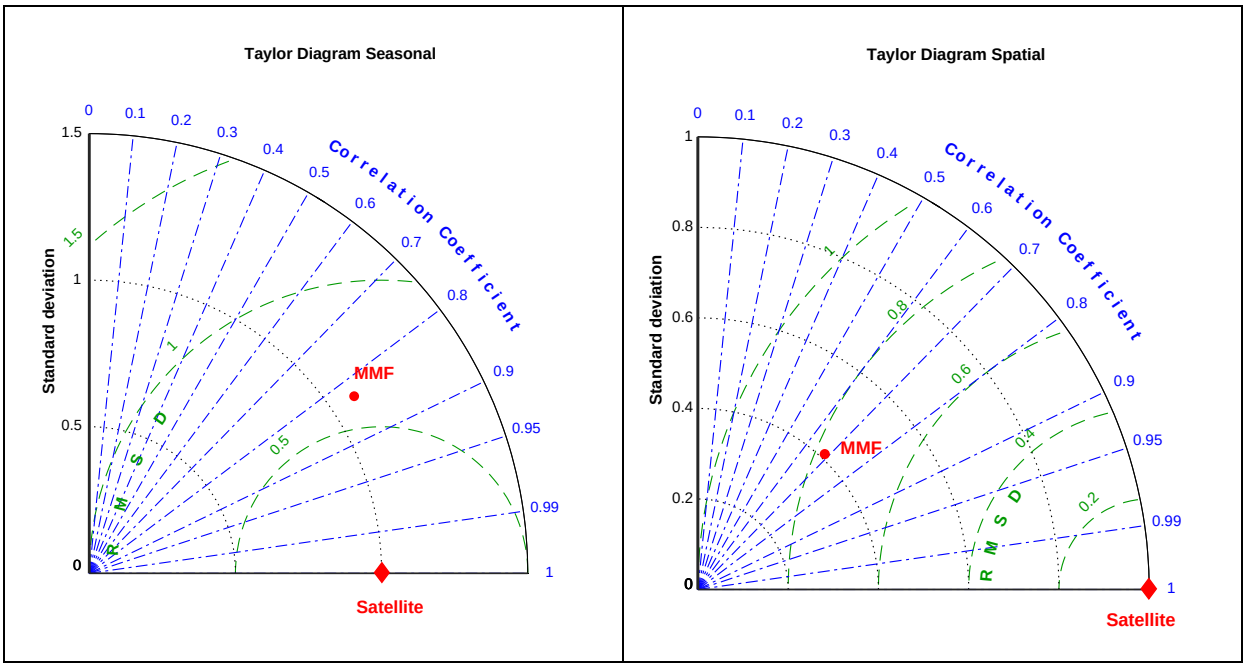

Figure 9. Left panel, Taylor Diagram of the monthly values comparison (shown in Fig. 8). Right panel, Taylor Diagram of the spatial distributions comparison (Fig. 7)

As already commented in the previous sections, for the North Sea, both the seasonal dynamic and the mean spatial distribution of PPR from satellite and from MMF are quite similar. Fig. 8 shows that the seasonal cycle in both estimates are quite highly correlated (r^2=0.83) and with very similar standard deviations. For the mean spatial distribution (right panel of Fig. 8), the correlation is 0.79 and MMF estimates have lower standard deviation (i.e., lower spatial heterogeneity) than satellite.

3.3 Mediterranean Sea

The Mediterranean Sea is another semi-enclosed basin with very limited connection with the open Atlantic Ocean. Through its only connection with the world´s ocean (the Strait of Gibraltar) an anti-estuarine circulation is established, with surface entrance of relatively warm and fresh Atlantic waters and a deep outflow of cooler, more saline Mediterranean waters. The excess evaporation with respect freshwater inputs (rivers + precipitation) in the basin interior makes it an essentially convective region where deep-waters are generated. All these characteristics make this basin an oligotrophic region with relatively low PPR levels with respect other EU regional seas.

3.3.1 Reference values

As for the other basins, table 3 shows a set of values for PPR in the Mediterranean Sea coming from different sources, field measurements, satellite estimates and model simulations.

Area	PPR (gC m^{-2} y^{-1}) ^{14}C	PPR (gC m^{-2} y^{-1}) MMF	PPR (gC m^{-2} y^{-1}) Satellite	Reference for the ^{14}C values
Med Sea	80-90	161(64)	180(107)	Sournia, 1973
Med Sea	62-81			Moutin & Raimbault, 1996
Eastern Med	137-150	126(38)	134(66)	Bethoux, 1989
Eastern Med	20.3			Dudgale & Wilkerson, 1988
Eastern Med	99			Moutin & Raimbault, 1996
Southern Adriatic	97.3	118(31)	242(33)	Boldrin et al., 2002
Southern Adriatic	110			Bianchi et al., 1999
Ionian	72	121(36)	151(121)	Bianchi et al., 1999
Ionian	63			Boldrin et al., 2002
Ionian	44-153			Moutin & Raimbault, 1996
Ionian	76-120			Casotti et al., 2003
Strait of Sicily	153	167(34)	192(42)	Moutin & Raimbault, 1996
North Aegean	85-120	152(36)	242(76)	Zervoudaki et al., 2006
Cretan Sea	59	144(26)	132(8)	Psarra et al., 2000
Western Med	100-120	226(45)	212(58)	Bethoux, 1989
Western Med	145			Moutin & Raimbault, 1996
Alboran Sea	175-321	301(65)	313(82)	Lohrenz et al., 1988

Alboran Sea	2 – 233			Macias et al., 2009
Catalan Sea	59 - 277	232(30)	212(39)	Estrada, 1989
Catalan Sea	55 – 328			Granata et al., 2004
Catalan Sea	147 – 365			Moran & Estrada, 2005
Algerian basin	68 – 232	238(42)	219(47)	Moran et al., 2001
Gulf of Lion	60 – 146	221(43)	273(62)	Gaudy et al., 2003
Gulf of Lion	140 – 150			Conan et al., 1998
Tyrrhenian Sea	145	199(32)	173(32)	Moutin & Raimbault, 1996
Tyrrhenian Sea	99 – 157			Decembrini et al., 2009
Ligurian Sea	86 – 232	209(34)	234(42)	Marty & Chiaverini, 2002
MEAN (range)	**131(90 - 172)**	**186(132 - 240)**	**207(155 - 259)**	

Table 3. Compilation of PPR values from different sources for the Mediterranean Sea

Mean values of all datasets show PPR levels corresponding to an oligotrophic environment, being lower than those reported for the Baltic or the North Sea above. The three used datasets (field measures, satellite and MMF) show comparable mean PPR values and a quite large SD, a reflection of the high spatial heterogeneity of PPR levels in this basin (see also discussion below). In order to understand better the relationship between the measured data and estimates in the table above, a scatter plot of the data is presented in Figure 10.

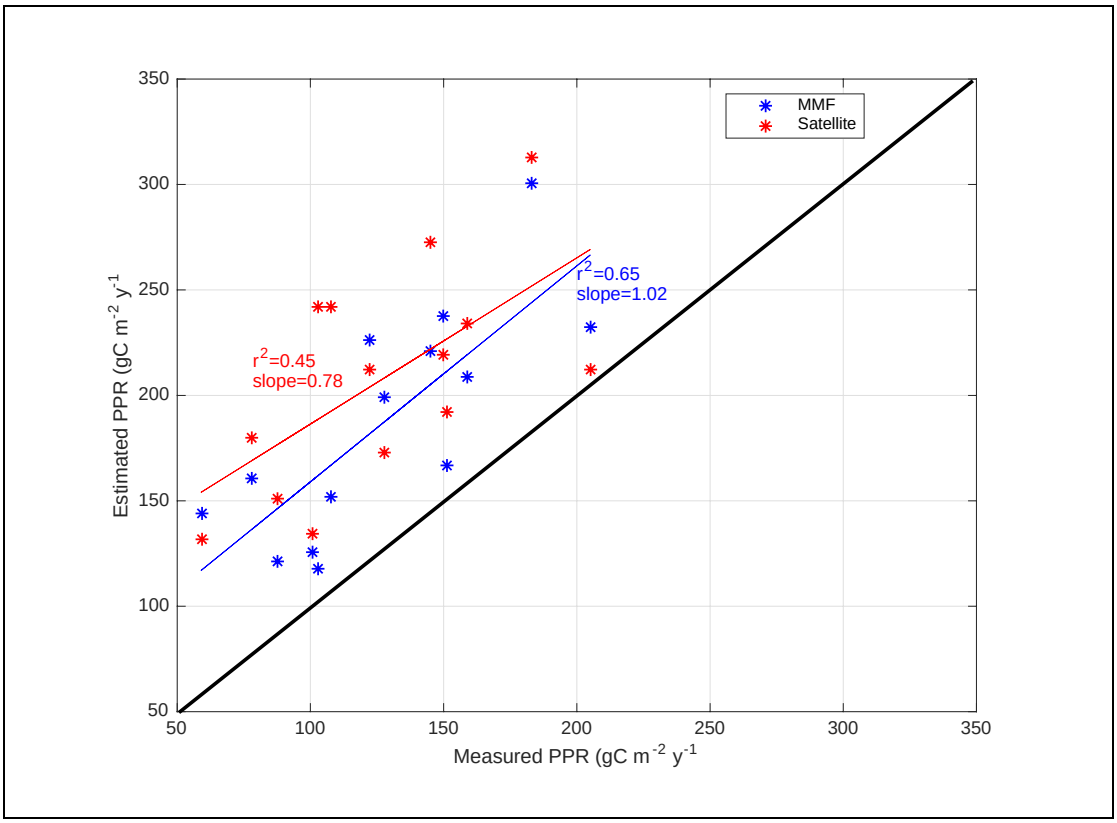

Figure 10. Measured PPR versus estimated PPR for the different regions in the Mediterranean Sea as shown in Table 3. The thick black line indicate the 1:1

Both estimates show values over the 1:1 line, indicating a positive bias, which is 59 gC m^{-2} y^{-1} for the MMF and 89 gC m^{-2} y^{-1} for the satellite. The correlation coefficient is significant for both estimates ($p<0.01$ for MMF and $p=0.014$ for satellite) although larger in the case of MMF. Also, the slope of the linear regression for MMF estimates is pretty close to 1 (see Fig. 10) indicating that the bias is consistent throughout the range of considered values.

In any case, this comparison is mostly qualitative as it is not fully accurate to compare individual measures with scattered spatial-temporal distribution with mean estimates for long-time periods. However the relative good agreement between the ranges of observed and estimated values and the fact that the slopes of the regression lines are close to 1 indicate that both satellite and MMF are good descriptors of PPR levels in the Mediterranean Sea.

3.3.2 Spatial patterns of PPR from satellite and MMF estimates

Fig. 11 shows the mean spatial distribution of PPR values in the Mediterranean Sea for the period 2005 -2012 computed from satellite estimates and by the MMF. In both cases there is a clear west to east gradient with higher values in the Alboran Sea and Gulf of Lion region and much lower in the eastern basin. This is the typical pattern of chlorophyll distribution in the Mediterranean (*e.g.*, Uitz et al., 2010) and follows the trophic gradient already known for this basin.

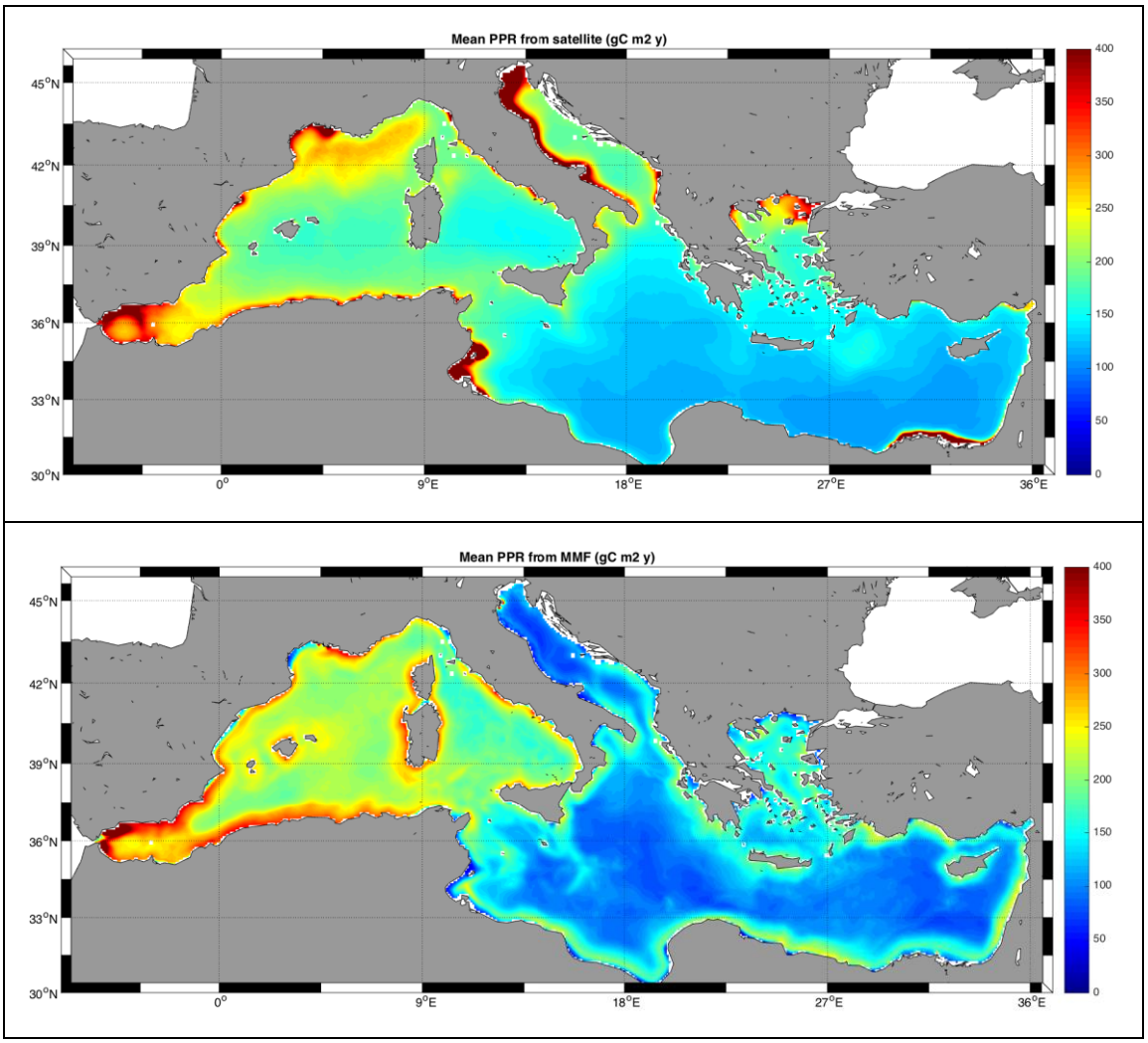

Figure 11. Mediterranean Sea PPR estimates. Upper panel, mean PPR estimated by remote sensing for the period 2005 – 2012. Lower panel, mean PPR estimated by the MMF for the period 2005 – 2012.

In spite of both maps showing similar patterns, there are also quite remarkable differences. PPR levels estimated by the satellites for the Adriatic Sea are much higher than those computed by the MMF. This discrepancy could be related with an underestimation of chlorophyll levels (and hence PPR) in the MMF (as discussed by Macias et al., 2019) or to an overestimation of such values by satellite imagery due to the particular optical characteristics of this area (i.e., high sediment loads from the Po outlet). Also, satellite estimates show a very high PPR area in the Gulf of Gabes region, a pattern not shown in the MMF map. It has already been shown that part of the primary productivity estimated by the satellite in this region is an artifact due to the very shallow depth of this area and the presence of bottom vegetation (*e.g.*, Jacquet et al, 1999).

3.3.3 Temporal PPR analysis from satellite and MMF

The mean monthly values of PPR for the entire Mediterranean Sea for both satellite and MMF estimates are shown in Fig. 12. In both datasets a clear seasonal cycle could be observed, with peak values in spring and minimum during late summer. The amplitude of

the seasonal signal and its phase agree quite well in both cases, although minimum levels are lower in the MMF computation. This feature could be related with the typical overestimation of chlorophyll values by satellite estimates for the ultra-oligotrophic regions of the Mediterranean Sea, particularly during non-bloom periods (*e.g.*, Uitz et al., 2010).

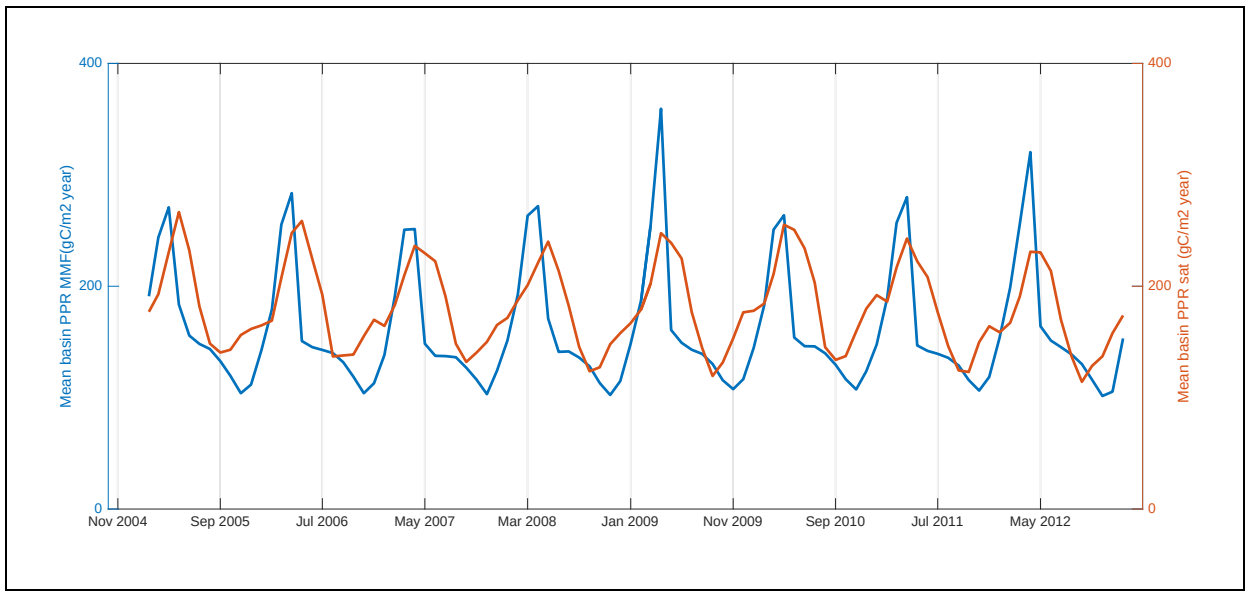

Figure 12. Mean monthly NPP (gC $m^{-2}y^{-1}$) for satellite and MMF estimates for the period 2005 – 2012.

3.3.4 Statistical comparison of PPR from satellite and MMF

Taylor Diagrams for the spatial and temporal comparisons of PPR estimates for the Mediterranean Sea are shown in Fig. 13.

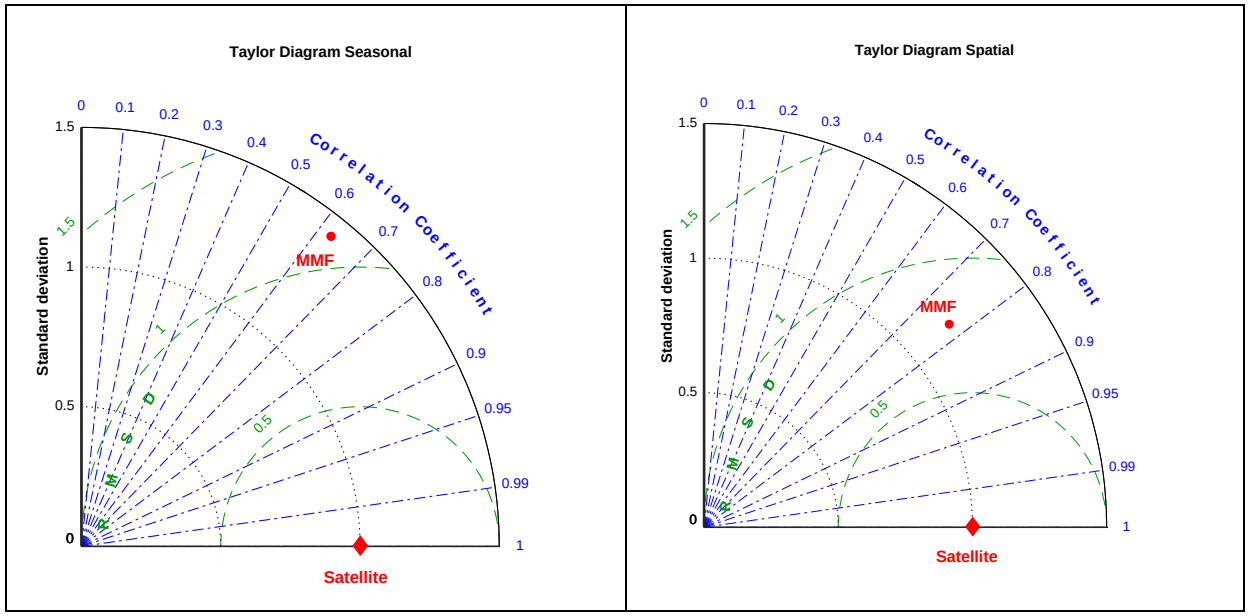

Figure 13. Left panel, Taylor Diagram of the monthly values comparison (shown in Fig. 12). Right panel, Taylor Diagram of the spatial distributions comparison (Fig. 11) (here the very shallow area <30m have been excluded as satellite estimates are typically not reliable there).

The comparison of monthly values (Fig. 13, left panel) indicates that both model and satellite agree quite well, with a correlation coefficient of 0.64. Standard deviation is larger in MMF than in the satellite estimates, indicating a slightly larger seasonal cycle in model computations.

Regarding spatial patterns comparison (Fig. 13, right panel), the correlation coefficient is even larger (0.77) and the standards deviations are very similar in satellite and model (please bear in mind that very shallow areas (<30m) are not included here).

This statistical analysis indicates that both datasets of PPR levels in the Mediterranean Sea are quite comparable. As discussed above, neither model nor satellite estimates are fully coincident with real values in the sea but in the case of this basin both provide a similar picture. This indicates that MMF computations of PPR in the Mediterranean Sea could be used as proxy for this ecosystem process with a reasonable level of confidence.

3.4 Black Sea

The Black Sea has unique natural conditions like a positive net freshwater balance, strong basin wide cyclonic circulation, and the so-called Rim Current, with well-exhibited western and eastern gyres. The Cold Intermediate Layer with temperatures less than 8°C exists in the sub-surface Black Sea's waters and over 90% of the basin deep water volume consists of anoxic water. Some of Europe's longest and largest rivers flow into it, including the Danube and the Dniepr. Fresh water from the rivers is spread along the shelf before entering the Rim Current and eventually is mixed with the waters from the basin interior. The interaction between the oxygen rich surface waters and the deep zones is limited by density stratification, which is amplified only under particular meteorological conditions, leading to a layered structure that affects the diversity of the organisms within the Black Sea (Murray et al., 1991).

Horizontally, two distinct regions can be outlined: one being the wide and shallow North-Western Shelf (< 200 m), the second being the deep sea, which is bounded by the 1500 m isobath. The latter is mostly isolated from the direct riverine inflow, which is known to be a key driver in the shelf. However, the mesoscale eddies evolve along the periphery of the basin, as a part of the Rim Current dynamic structure. They effectively link coastal hydrodynamic and biogeochemical processes to those in the deep sea and thus provide a mechanism for two-way transport between near shore and offshore regions. These two regions show pronounced physical and biological differences (McQuatters-Gollop et al., 2008). Climate affects the Black Sea via atmospheric forcing and riverine inflow, which has been demonstrated to be a significant factor for the overall water balance and basin-scale circulation (Miladinova et al., 2018). Miladinova et al. (2020) suggested that the bloom seasonality is homogeneous across geographic locations of the Black Sea inner basin, with the strongest bloom occurring in winter (February-March), followed by weaker bloom in

spring (April-May), summer deep biomass maximum (June-September) and a final bloom in autumn (October-November).

The Black Sea ecosystem underwent a stage of eutrophication in the 1970s and 2000s, which manifested itself in high levels of chlorophyll a, phytoplankton biomass, primary production and low oxygen content. It is established that the Black Sea ecosystem has gone through three different stages. They are: a pre-eutrophication (1960-1970), eutrophication (1980-1995) and post-eutrophication period after 2005. The duration of these periods and the transitional periods between them vary in the studies (Yunev et al., 2011; Oguz et al., 2006; Mikaelyan et al., 2013). However, there is a clear consensus on the Black Sea ecosystem evolution in the recent six-five decades. According to the findings in Yunev et al. (2011), by the end of the 1980s and the early 1990s, the value of the annual primary production in the inner part of the sea increased from 63 ± 18 g C m–2 y–1 (in the 1960s) up to 135 ± 30 g C m–2 y–1. On the contrary, after 1993, mainly because of reduced runoff of biogenic substances into the Black Sea from land-based sources, there was a decrease in the annual production of phytoplankton in the inner basin, which is about 105 g C m–2 y–1 in 2008. Mikaelyan et al. (2013) estimated that the averaged depth-integrated phytoplankton biomass increased 6 times from 3.3 g C m−2 in 1969–1983, to 19.6 g C m−2 during 1984–1995 and decrease down to 10.6 g C m−2 in 1996–2008, what was still 3 times higher than during 1969–1983. Thus, we have to keep in mind the fact for which period the PPR values are estimated.

3.4.1 Reference values

Field data found in the literature are reported in table 4 below. To compute the mean and SD of those data, individual values reported within the used papers have been used (N=41). The analysis of MODIS-Aqua data for 2003–2013 and SeaWiFS data for 1998–2007 indicates that Oceancolor Level 2 and 3 chlorophyll data contain systematic inconsistencies in the Black Sea basin, which are related to the effect of cloud shadows (Kubryakov et al., 2016). Zones with very high chlorophyll concentration are observed to the north of large clouds. Most of these errors are observed in late autumn through the winter months, when the Sun is low in the Northern Hemisphere. Color remote sensing imagery for the Black Sea is typically very sparse due to the high cloud coverage in this area. Also, the very particular physical and biogeochemical vertical distributions in the basins make standard global satellite products not applicable here. As explained Section 2.2, this has been partly circumvented by the use of a semi-analytical bio-optical algorithm to compute inherent optical properties that should lead to a better estimate of phytoplankton and representation of the light field in the water column.

Area	PPR (gC m^{-2} y^{-1}) ^{14}C	PPR (gC m^{-2} y^{-1}) MMF	PPR (gC m^{-2} y^{-1}) Satellite	Reference for the ^{14}C values
South-west + Central East	88-271	80 (17)	121 (25)	McCarthy et al., 2007
South East shelf	104 - 206	75(18)	141(33)	Agirbas et al., 2014
South East open waters	46 - 193	64(4)	109(5)	Agirbas et al., 2014
Central Black Sea	135	65(6)	108(4)	Yunev, 2011
Central Black Sea	110			Yunev et al., 2002
MEAN (range)	**189(63 - 315)**	**71(64 - 78)**	**119(104 - 134)**	

Table 4. Compilation of PPR values from different sources for the Black Sea

From the comparison of values in table 4, it seems that MMF estimates are lower than reported values, while satellite estimates are closer to measured values. It is worth to note that the in-situ data of McCarthy et al. (2007) cover 1998-2001, Agirbas et al. (2014) – 03-12/2010, Yunev, 2011 – 1980-1993 and Yunev, 2002 - 1980-1996.

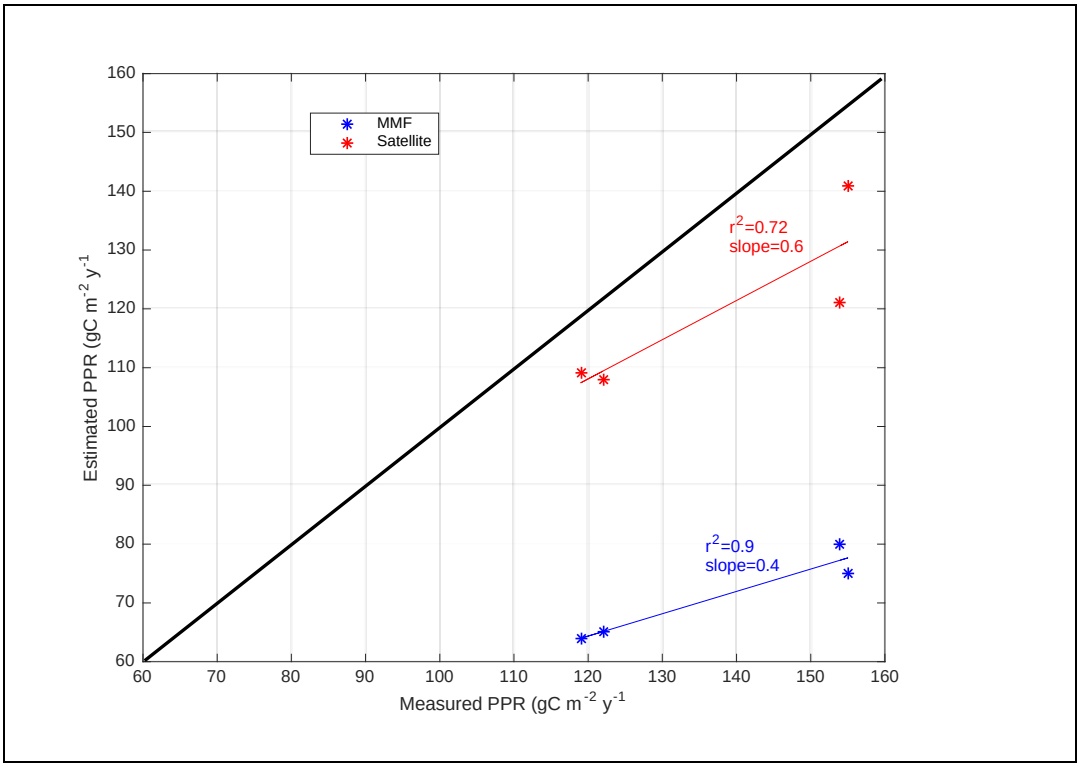

Figure 14. Measured PPR versus estimated PPR for the different regions in the Black Sea as shown in Table 4. The thick black line indicate the 1:1

The scatter plot of measured vs. estimated PPR values (Fig. 14) indicates that both estimates (satellite and MMF) underestimate measured values. Mean bias for MMF is 66 gC/m^{2}y while for satellite this value is 18 gC/m^{2}y. In both cases, however, there is a very high correlation between the different datasets reaching 90% for the MMF.

Another dataset of estimated PPR in the Black Sea could be found in the work by Deminov (2008). In that analysis, the author used empirical relationships between chlorophyll-a and in situ PPR during 1973 – 1997 to create climatologies for 10 different regions within the basin. The annual mean value for those 10 regions of the Black Sea and the corresponding estimates from the MMF and satellite are provided in table 5 below. Obviously, in-situ estimates are higher than model results. A reason for the discrepancy between the data and the model includes the different time periods for PPR assessment. Another reason for the discrepancy is the lack of measurements during the winter period (December-February), when values of PPR are lower.

Region	Annual mean by Deminov (2008) (gC m^{-2} y^{-1})	Annual mean by MMF (gC m^{-2} y^{-1})	Annual mean by sat (gC m^{-2} y^{-1})
Danube	381	254	262
NW shelf	160	123	209
SW shelf	266	131	194
NW continental slope	115	122	170
SW continental slope	149	110	133
Eastern shelf	101	83	141
Eastern continental slope	102	66	115
Western continental slope	111	102	112
Eastern deep waters	99	61	108
Western deep waters	94	72	108

Table 5. Compilation of mean PPR values from Deminov (2008) and the estimates for the same regions by the MMF and satellite data.

The scatter plot of the values shown in table 5 above indicates a sub-estimation of the PPR values by 46 gC m^{-2} y^{-1} by the MMF and of 39 gC m^{-2} y^{-1} by the satellite data (Figure 15). However, the correlation coefficient is very high (r^2=0.85 for MMF and r^2=0.79 for satellite) and highly significant ($p<0.01$ for both estimates).

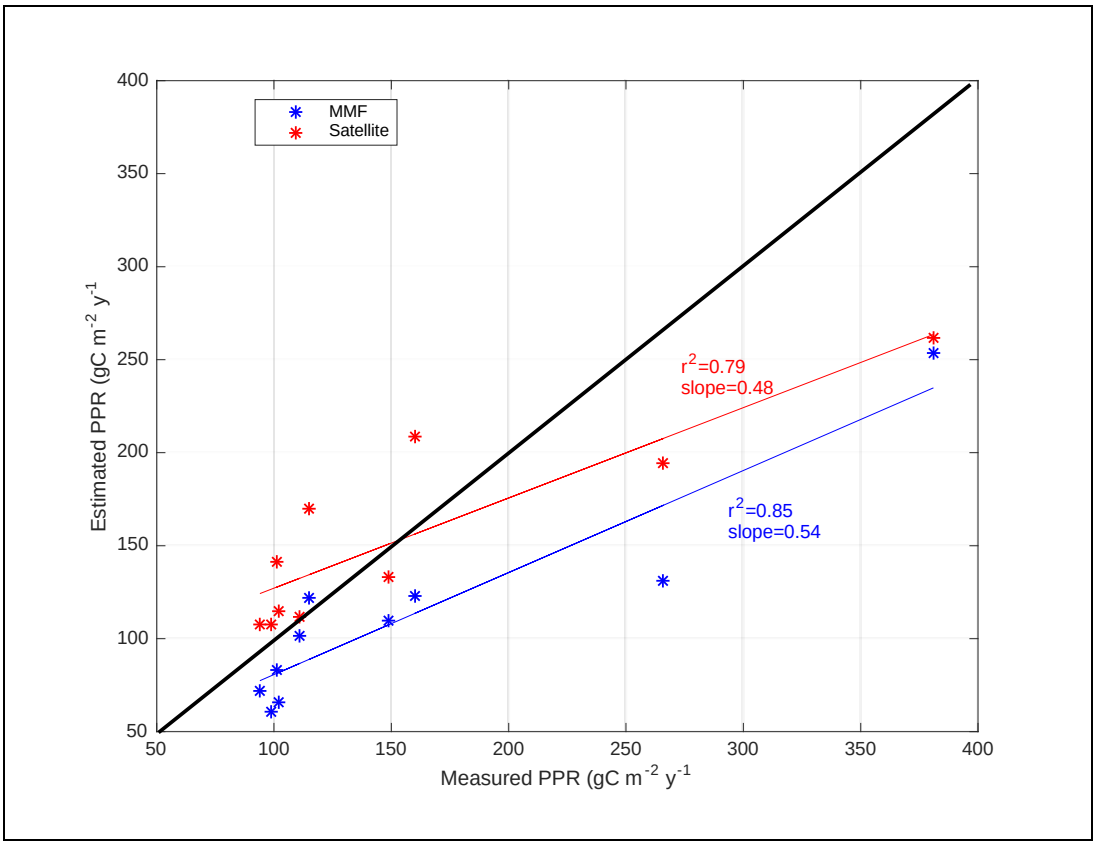

Figure 15. Scatter plot of mean annual values for different Black Sea regions from Deminov (2008) and different estimates (data shown in table 5).

In this case, we can say both satellite and MMF are good proxies of measured PPR in the Black Sea basin. Hence, we can use both estimates to explore the spatial-temporal patterns of this variable in the region.

3.4.2 Spatial patterns of PPR from satellite and MMF estimates

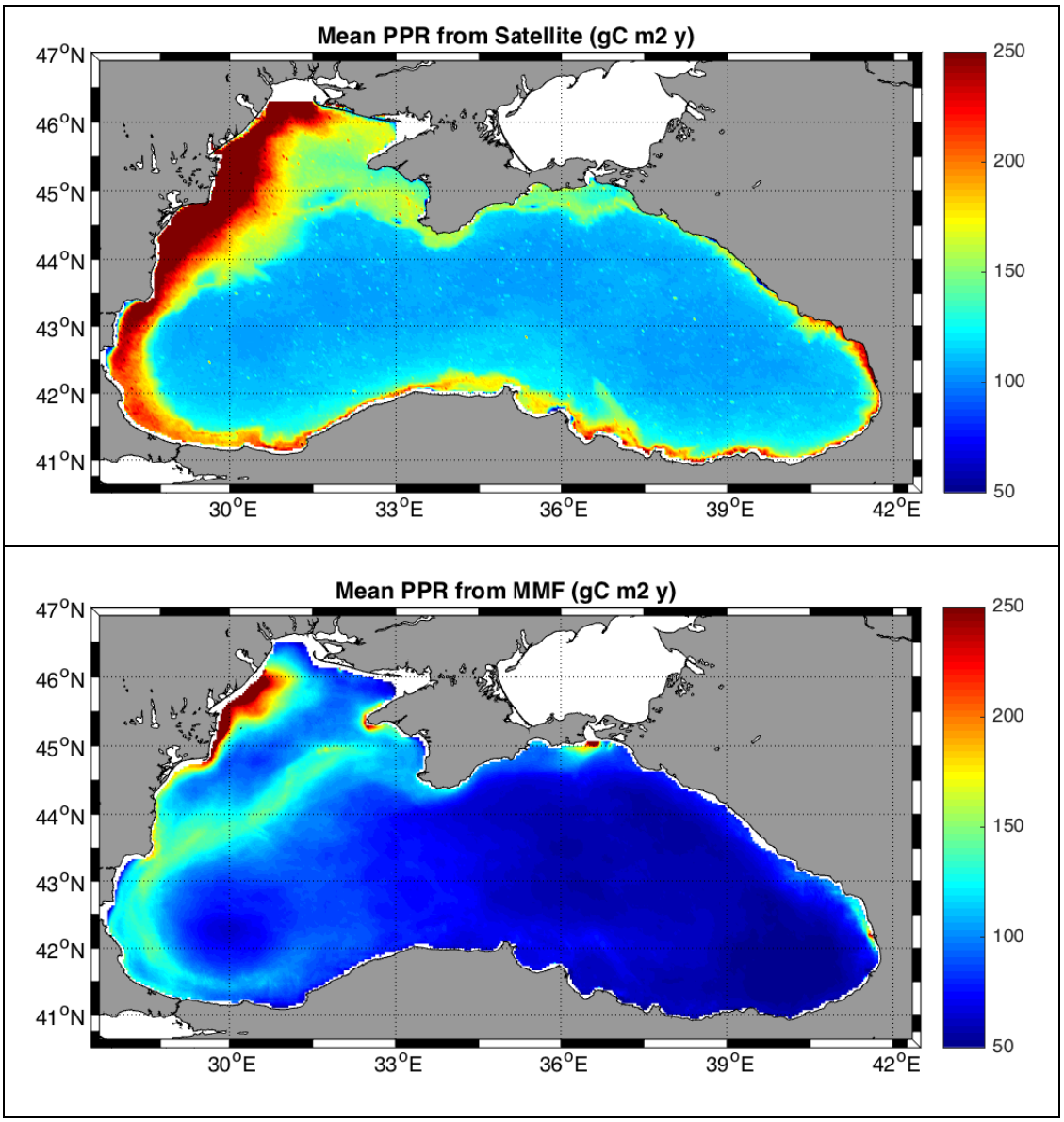

Figure 16. Black Sea PPR estimates. Upper panel, mean PPR estimated by remote sensing for the period 1998 – 2003. Lower panel, mean PPR estimated by the MMF for the period 1998 – 2003.

Both satellite and MMF estimates, shows a very similar picture of the distribution of PPR in the Black Sea (Fig. 16). The maximum levels of primary production are attained in the NW Shelf, nearby the outlet of the Danube river. Medium levels extend along the shelf break area, especially in the Western and SW regions while the open sea region is characterized by very low PPR values. In this case, both maps in Fig. 16 use the same scale for the colour bar, indicating the close match between the two estimates of the mean PPR in the basin.

3.4.3 Temporal PPR analysis from satellite and MMF

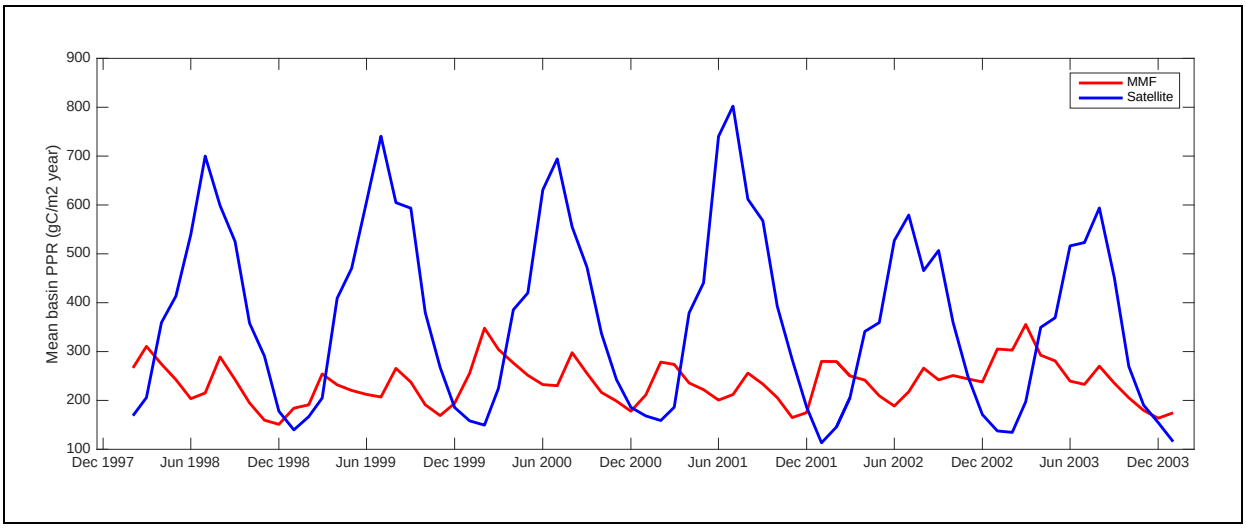

Figure 17. Mean monthly PPR (gC $m^{-2}y^{-1}$) for satellite and MMF estimates for the period 1998 – 2003.

However, and even if mean PPR within the Black Sea are very similar in MMF and satellite, their seasonal cycle is quite different (Fig. 17). Satellite estimates shows a very marked and large seasonal cycle with maximum values (700 gC $m^{-2}y^{-1}$) in summer and minimum (200 gC $m^{-2}y^{-1}$) during winter. The MMF estimates are less variable, with maximums located in late spring and fall (at around 300 gC $m^{-2}y^{-1}$) and minimum in winter (200 gC $m^{-2}y^{-1}$).

As discussed in the introduction, ocean colour remote sensing information for the Black Sea is quite uncertain and, hence, the same applies to the PPR derived from those images. For that reason, we decided to use again Deminov (2008) dataset, as those authors provided a seasonal PPR cycle for the 10 regions analysed (shown in table 5). Figure 18 below show the Deminov monthly values, the MMF estimates and the satellite ones for those 10 regions.

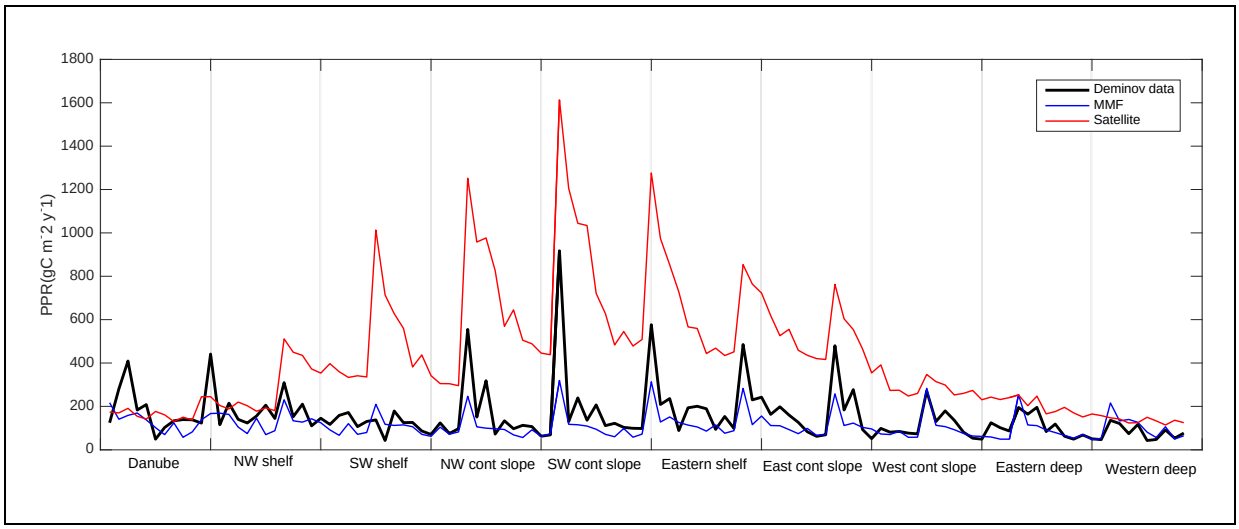

Figure 18. Monthly PPR estimates from Deminov dataset, MMF and satellite for the ten regions included in Deminov (2008) and shown in table 5.

In this case, it could be seen that MMF estimates are much closer to Deminov (2008) reported values, with a mean bias of 59 gC $m^{-2}y^{-1}$and an overall correlation coefficient of 0.6. Satellite

estimates are further apart, with a mean bias of 281 gC $m^{-2}y^{-1}$ and a correlation coefficient of just 0.3. This later comparison indicates that MMF could be better at capturing the actual PPR seasonality in the Black Sea than remote sensing products.

3.4.4 Statistical comparison of PPR from satellite and MMF

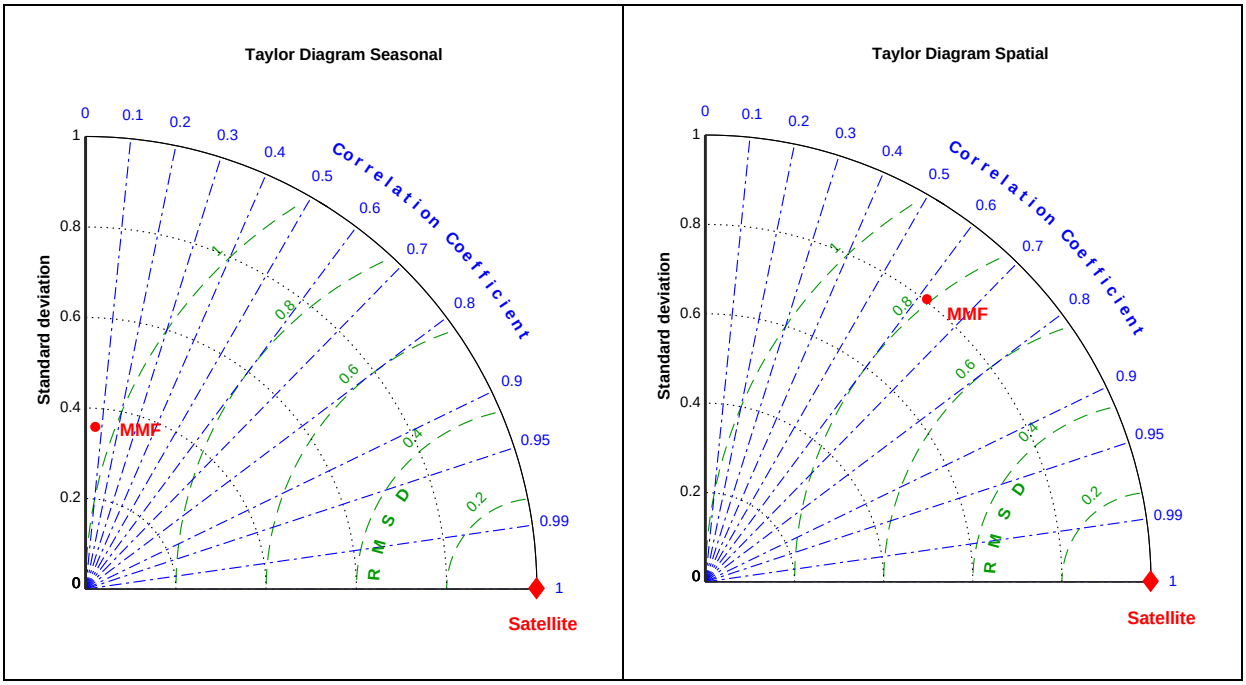

Figure 19. Left panel, Taylor Diagram of the monthly values comparison (shown in Fig. 17). Right panel, Taylor Diagram of the spatial distribution comparison (Fig. 16).

As already advanced above, there is no significant correlation between the seasonal dynamic of PPR estimated by satellite and the one estimated by the MMF (Fig. 19, left panel). For the spatial distribution, however, the correlation coefficient is around 0.63 and both estimates show similar standard deviations, indicating a comparable level of spatial heterogeneity.

4 Summary

As in many occasions in marine sciences, it is impossible to know the true value of the primary production rates (PPR) in EU waters. There exist different approaches based on diverse methodologies (water incubation, remote sensing and numerical models) all with flaws and strength. As evaluating the absolute error (difference between true value and estimates) is not possible (because the true value is not known) the only thing we can do is to compare different estimates among themselves and evaluate their relative error. If for a specific region all three different estimates are close and within their variability range, we can be more confident on such estimates (as their sources of error are different).

However, the main objective of the present report is to evaluate the usefulness of the MMF estimates to represent PPR levels in EU marine ecosystems. For that reason, we put major emphasis in the validation of MMF estimates against the other two datasets. In general we can say MMF underestimates the range of measured PPR (except for the Mediterranean Sea) but it represent quite well the seasonal dynamics of PPR presented by either satellite estimates (Baltic, North Sea and Mediterranean) or by field estimates (Black Sea). Regarding spatial distributions, both MMF and satellite seems to agree except for the Baltic Sea.

The major highlights for each of the EU basins could be listed as the following:

a) Baltic Sea:

- MMF underestimates measured values and satellite estimates. However, mean basin-wide integrated PPR from MMF corresponds to previous estimates from field data.
- Good representation of the seasonal cycle (i.e., good agreement between MMF and satellite)
- MMF and satellite spatial distributions do not agree (although satellite estimates are problematic in this basin)

b) North Sea:

- MMF underestimates measured values and satellite estimates (but in this case it is closer than in the Baltic Sea)
- Both seasonal cycle and spatial distribution in MMF and satellite are quite similar

c) Mediterranean Sea:

- MMF and satellite values are all quite close to measured PPR
- Spatial distribution quite similar in MMF and satellite except in very shallow areas (<30m) where satellites usually have issues to calculate chlorophyll
- Seasonal cycle very similar in MMF and satellite

d) Black Sea:

- MMF and satellite both underestimate in-situ values. Here we must point that most of the in-situ data was measured in early 1990s, when the Black Sea was on a more eutrophic state than in the mid-2000s (when both satellite and MMF estimates are calculated)
- There is a quite good agreement spatially between Deminov (2008) mean values (10 regions) and MMF/satellite estimates
- The spatial distribution of integrated PPR is quite similar in MMF and satellite
- The seasonal cycle in both MMF and satellite estimates is completely different. However, MMF results correlate better with Deminov (2008) monthly values for the 10 analysed regions than the satellite estimates

References

Anderson, T.R., Martin, A.P., Lampitt, R.S., Trueman, C.N., Henson, S.A., Mayor, D.J., Handling, 2018. Quantifying carbon fluxes from primary production to mesopelagic fish using a simple food web model. Jason, Link (Ed.), Quantifying carbon fluxes from primary production to mesopelagic fish using a simple food web model. ICES J. Mar Sci. https://doi.org/10.1093/icesjms/fsx234.

Abraham, J.P., Baringer, M., Bindoff, N.L., Boyer, T., Cheng, L.J., et al. 2013. A review of global ocean temperature observations: Implications for ocean heat content estimates and climate change. Reviews of Geophysics, 51(3), 450-483, doi: 10.1002/rog.20022.

Agirbas, E., Muzaffer-Feyzioglu, A., Kopuz, U., 2014. Seasonal Changes of Phytoplankton Chlorophyll a, Primary Production and their Relation in the Continental Shelf Area of the South Eastern Black Sea. Turkish J. Fish. Acq. Sci., 14, 713-726.

Andersen, J.H., Carstensen, J., Conley, D.J., Dromph, K., Fleming-Lehtinen, V., Gustafsson, B.G., Josefson, A.B., Norkko, A., Villnäs, A., Murray, C., 2017. Long-term temporal and spatial trends in eutrophication status of the Baltic Sea. Biological Reviews, 92(1), 135-149, doi: 10.1111/brv.12221

Andrushaitis, G., Andrushaitis, A., Bitenieks, Y., Priede, S., Lenshs, E., 1992. Organic carbon balance of the Gulf of Riga. In: Swed. Hydrol. Meteor. Inst. Rep., Proc. 17th CBO Conf., Norrköping, p.1009.

Anon, 1993. North Sea Quality Status Report. North Sea Task Force.

Behrenfeld, M.J., Falkowski, P.G., 1997. Photosynthetic rates derived from satellite-based chlorophyll concentration. Limnol. Oceanogr. 42, 1–20. https://doi.org/10.4319/lo.1997.42.1.0001.

Behrenfeld, M.J., O'Malley, R.T., Boss, E.S., Westberry, T.K., Graff, J.R., Halsey, K.H., Milligan, A.J., Siegel, D.A., Brown, M.B., 2016. Revaluating ocean warming impacts on global phytoplankton. Nat. Clim. Change 6, 323–330. https://doi.org/10.1038/nclimate2838.

Bethoux, J.P., 1989. Oxygen consumption, new production, vertical advection and environmental eveolution in the Mediterranean Sea. Deep-Sea Research, 36, 760 – 780.

Bianchi, F., Boldrin, A., Civitarese, G., Del Negro, P., Giordani, P., Malaguti, A., Socal, G., Rabitti, S., Turchetto, M. 1999. Biogenic particulate matter and primary productivity in the Southern Adriatic and Northern Ionian seas, in: 4th MTP-Workshop MATER., Volume, 120-121, Les Presses Litteraires, Perpignan (France).

Boldrin, A., Miserocchi, S., Rabitti, S., Turchetto, M., Balboni, V., Socal, G. 2002. Particulate matter in the southern Adriatic and Ionian Sea: characterisation and downward fluxes. J. Mar. Syst., 33-34, 389-410.

Bopp, L., Legendre, L., Monfray, P. 2002. La pompe à carbone va-t-elle se gripper. La Recherche, 355, 48-50

Bricaud, A., Babin, M., Morel, A., Claustre, H., 1995. Variability in the chlorophyll-specific absorption coefficients of natural phytoplankton: Analysis and parameterization. *J. Geophys. Res.*, 100, 13321-13332.

Bruggeman, J., Bolding, K., 2014. A general framework for aquatic biogeochemical models. Environ. Modell. Software 61, 249–265.

Burchard, H., Bolding, K., 2002. GETM, A General Estuarine Transport Model. European Commission, Ispra, Italy.

Butenschon, M., Clark, J., Aldridge, J.N., Allen, J.I., Artioli, Y., Blackford, J., *et al.* 2016. ERSEM 15.06: a generic model for marine biogeochemistry and the ecosystem dynamics of the lower trophic levels. Geosci. Model Dev. 9(4), 1293-1339.

Campbell J., Antoine D., Armstrong R., Arrigo K., Balch W., Barber R., Behrenfeld M., Bidigare R., Bishop J., Carr M.-E., Esaias W., Falkowski P., Hoepner N., Iverson R., Keifer D., Lohrenz S., Marra J., Morel A., Ryan J., Vedemikov V., Waters K., Yentsch C., Yoder J., 2002, Comparison of algorithms for estimating ocean primary production from surface chlorophyll, temperature, and irradiance , Global Biogeochem. Cy., 16 (3), 74–75, http://dx.doi.org/10.1029/2001GB001444.

Carr, M.E., Friedrichs, M.A.M., Schmeltz, M., Aita, M.N., Antoine, D., Arrigo, K.R., Asanuma, I., Aumont, O., Barber, R., Behrenfeld, M., Bidigare, R., Buitenhuis, E.T., Campbell, J., Ciotti, A., Dierssen, H.,

Dowell, M., Dunne, J., Esaias, W., Gentili, B., Gregg, W., Groom, S., Hoepffner, N., Ishizaka, J., Kameda, T., Le Quere, C., Lohrenz, S., Marra, J., Melin, F., Moore, K., Morel, A., Reddy, T.E., Ryan, J., Scardi, M., Smyth, T., Turpie, K., Tilstone, G., Waters, K., Yamanaka, Y., 2006. A comparison of global estimates of marine primary production from ocean color. *Deep-Sea Research II,* 53, 741–770.

Cassoti, R., Landofi, A., Brunet, C., D'Ortenzio F., Mangoni, O., Ribera d'Alcalá, M., Denis, M. 2003. Composition and dynamics of the phytoplankton of Ionian Sea (eastern Mediterranean). J. Geophys. Res., 108, 8116.

Conan, P., Pujo-Pay, M., Raimbault, P., Leveau, M. 1998. Variabilité hydrologique et biologique du golfe du Lion. II. Productivité sur le bord interne du courant. Oceanol. Acta, 21, 767-781.

Cummings, J.A., Smedstad, O.M. 2013. Variational Data Assimilation for the Global Ocean. In: Park SK, Xu L, editors. Data Assimilation for Atmospheric, Oceanic and Hydrologic Applications (Vol. II). Berlin, Heidelberg: Springer Berlin Heidelberg, 2013. p. 303-343.

D'Alimonte, D., Zibordi, Berthon, J.-F., Canuti, E., Kajiyama, T., 2012. Performance and applicability of bio-optical algortihms in different European seas. Remote Sens. Environ., 124, 402-412.

Decembrini, F., Caroppo, C., Azzaro, M. 2009. Size structure and production of phytoplankton community and carbon pathways channelling in the Southern Tyrrenian Sea (Western Mediterranean). Deep-Sea Res. Pt. II, 56, 687-699.

Demidov, A.B. 2008. Seasonal Dynamics and Estimation of the Annual Primary Production of Phytoplankton in the Black Sea. Oceanology 5(48): 664–678. doi: 10.1134/S0001437008050068

Duarte, C.M., Cebri.n, J., 1996. The fate of marine autotrophic production. Limnol. Oceanogr. 41, 1758–1766. https://doi.org/10.4319/lo.1996.41.8.1758.

Dugdale, R.C., Wilkerson, F.P., 1988. Nutrient sources and primary production in the eastern Mediterranean. Oceanol. Acta, Special Issue, 179 - 184.

Emeis, K., van Beusekom, J., Callies, U., Ebinghaus, R., Kannen, A., Kraus, G., Kröncke, I., Lenhart, H., Lorkowski, I., Matthias, V., Möllmann, C., Pätsch, J., Scharfe, M., Thomas, H., Weisse, R., & Zorita, E. 2015. The North Sea — A shelf sea in the Anthropocene. Journal of Marine Systems, 141, 18-33. doi:10.1016/j.jmarsys.2014.03.012.

Estrada, M. 1996. Primary production in the northwestern Mediterranean. Sci. Mar., 60(Suppl. 2), 55-64.

Finenko, Z.Z., Suslin, V.V., and I.V. Kovaleva, 2014: Seasonal and long-term dynamics of the chlorophyll concentration in the Black Sea according to satellite observations, Oceanology 54(5), 596-605, DOI: 10.1134/S0001437014050063

Fransz, H.G., Gieskes, W.W.C., 1984. The unbalance of phytoplankton and copepods in the North Sea. Rapports et proces verbaux des reunions Cons.perm.int. Explor. Mer 183, 218-225.

Friedland, R., Stips, A., Grizzetti, B., de Roo, A., Lessin, G. 2020. Report on the bio-geochemical model of the North-Western European Shelf, Publications Of-fice of the European Union, Luxembourg, ISBN 978-92-76-17866-8, doi:10.2760/78173, JRC120213.

Friedrichs, M.A.M., Carr, M.-E., Barber, R.T., Scardi, M., Antoine, D., Armstrong, R.A., Asanuma, I., Behrenfeld, M.J., Buitenhuis, E.T., Chai, F., Christian, J.R., Ciotti, A.M., Doney, S.C., Dowell, M.D., Dunne, J., Gentili, B., Gregg, W.W., Hoepffner, N., Ishizaka, J., Kameda, T., Lima, I., Marra, J., Mélin, F., Moore, J.K., Morel, A., O'Malley, R.T., O'Reilly, J.E., Saba, V.S., Schmeltz, M., Smyth, T.J., Tjiputra, J., Waters, K., Westberry, T.K., Winguth, A., 2009. Assessing the uncertainties of model estimates of primary productivity in the tropical Pacific Ocean. *J. Mar. Sys*., 76, 113-133.

Ford, D.A., Van der Molen, J., Hyder, K., Bacon, J., Barciela, R., Creach, V., *et al.* 2017. Observing and modelling phytoplankton community structure in the North Sea. Biogeosciences. 14(6):1419-1444.

Galbraith, E.D., Martiny, A.C., 2015. A simple nutrient-dependence mechanism for predicting the stoichiometry of marine ecosystems. Proc. Natl. Acad. Sci. USA 112 (27), 8199–8204.

Gavin H.Tilston, G.H., Taylor, B.H., Blondeau-Patissier, D., Powell, T., Grooma, S.B., Rees, A.P., Lucas, M.I. 2015. Comparison of new and primary production models using SeaWiFS data in contrasting hydrographic zones of the northern

North Atlantic. Remote Sensing of the Environment, 156, 473-489. Doi: 10.1016/j.rse.2014.10.013

Gaudy, R., Youssara, F., Diaz, F., Raimbault, P. 2003. Biomass, metabolism and nutrition of zooplankton in the Gulf of Lions (NW Mediterranean). Ocanol. Acta, 26, 357-372.

Granata, T., Estrada, M., Zika, U., Merry, C. 2004. Evidence for enhanced primary production resulting from relative vorticity induced upwelling in the Catalan Current. Sci. Mar., 68(S1), 113-119.

Gräwe, U., Holtermann, P., Klingbeil, K., Burchard, H. 2015. Advantages of vertically adaptive coordinates in numerical models of stratified shelf seas, Ocean Modelling, 92, 56-68, https://doi.org/10.1016/j.ocemod.2015.05.008.

Grizzeti, B., Vigiak, O., Udias, A. Aloe, A. Zanni, M. Bouraoui, F. Pistocchi, A., Dorati, C. Friedland, R. De Roo, A. Benitez, Sanz C. Leip, A. Bielza, M. Submitted. How EU policies could reduce nutrient pollution in European inland and coastal waters? Global Environmental Change.

Hays, G., Richardson, A., Robinson, C., 2005. Climate change and marine plankton. Trends Ecol. Evol. 20, 337–344. https://doi.org/10.1016/j.tree.2005.03.004

Hickman, A.E., Moore, C.M., Sharples, J., Lucas, M.I., Tilstone, G.H., Krivtsov, V., Holligan, P.M. 2012. Primary production and nitrate uptake within the seasonal thermocline of a stratified shelf sea. Mar Ecol Prog Ser 463:39-57. https://doi.org/10.3354/meps09836

Howarth R.W., Michaels A.F. (2000) The Measurement of Primary Production in Aquatic Ecosystems. In: Sala O.E., Jackson R.B., Mooney H.A., Howarth R.W. (eds) Methods in Ecosystem Science. Springer, New York, NY. https://doi.org/10.1007/978-1-4612-1224-9_6

Jaquet, J. M. Tassan, S. Barale, V. and Sarbaji, M. (1999) Bathymetric and bottom effects on CZCS chlorophyll-like pigment estimation: data from the Kerkennah shelf (Tunisia), International Journal of Remote Sensing, vol. 20, no.7, pp. 1343–1362.

Janssen, F., Schrum, C., Backhaus, J.O., 1999. A climatological data set of temperature and salinity for the Baltic Sea and the North Sea. Dtsch. Hydrogr. Zeitschrift 51, 5–245. https://doi.org/10.1007/bf02933676

Joint, I., Pomroy, A., 1993. Phytoplankton biomass and production in the southern North Sea. Marine Ecology Progress Series, 99, 169-182.

Joiris, C., Billen, G., Lancelot, C., Daro, M.H., Mommarts, J.P., Bertels, A., Bossicart, M., Nijs, J., 1982. A budget of carbon cycling in Belgian coastal zone: relative role of zooplankton, bacterioplankton and benthos in the utilization of primary production. Netherland Journal of Sea Research 16, 260–275.

Kubryakov, A. A., S.V. Stanichny, A. G. Zatsepin, and V. V. Kremenetskiy, 2016: Long-term variations of the Black Sea dynamics and their impact on the marine ecosystem, Journal of M arine Systems, Volume 163, 2016, Pages 80-94, doi.org/10.1016/j.jmarsys.2016.06.006.

Lee, Z.P., Carder, K.L., and Arnone, R.A., 2002. Deriving inherent optical properties from water color: a multi-band quasi-analytical algorithm for optically deep waters. *Appl. Opt.*, 41, 5755-5772.

Lessin, G., Raudsepp, U., Stips, A., 2014. Modelling the influence of Major Baltic Inflows on near-bottom conditions at the entrance of the Gulf of Finland. PLoS One 9, e112881–e112881. https://doi.org/10.1371/journal.pone.0112881

Lohrenz, S., Wiesenburg, D., Depalma, I., Johnson, K., Guftanson, D. 1988. Interrelationships among primary production, chlorophyll and environmental conditions in frontal regions of the western Mediterranean Sea. Deep-Sea Res. 35, 793 – 810.

Longhurst, A.R., Glen Harrison, W., 1989. The biological pump: profiles of plankton production and consumption in the upper ocean. Prog. Oceanogr. 22, 47–123. https://doi.org/10.1016/0079-6611(89)90010-4.

Longhurst, A., Sathyendranath, S., Platt, T., Caverhill, C., 1995. An estimate of global primary production in the ocean from satellite radiometer data, *Journal of Plankton Research*, 17, 1245-1271.

Macias, D., Navarro, G., Bartual, A., Echevarria, F., Huertas, I.E. 2009. Primary production in the Strait of Gibraltar: Carbon fixation rates in relation to hydrodynamic and phytoplankton dynamics. Estuarine, Coast. Shelf Sci., 93, 197-210.

Macías, D., García-Gorríz, E., Piroddi, C., Stips, A., 2014a. Biogeochemical control of marine productivity in the Mediterranean Sea during the last 50 years. Global Biochem. Cycles 28, 897–907.

Macías, D., Stips, A., Garcia-Gorriz, E., 2014b. The relevance of deep chlorophyll máximum in the open Mediterranean Sea evaluated through 3D hydrodynamic-biogeochemical coupled simulations. Ecol. Model. 281, 26–37.

Macías, D., Garcia-Gorriz, E., Stips, A., 2015. Productivity changes in the Mediterranean Sea for the twenty-first century in response to changes in the regional atmospheric forcing. Front. Mar. Sci. 2 (79).

Macías, D., Huertas, I.E., Garcia-Gorriz, E., Stips, A., 2019. Non-Redfieldian dynamics driven by phytoplankton phosphate frugality explain nutrient and chlorophyll patterns in model simulations for the Mediterranean Sea. Prog. Ocean., 173, 37-50.

Marty, J.C., Chiaverini, J. 2002. Seasonal and interannual variations in phytoplankton production at DYFAMED time-series station, northwestern Mediterranean Sea. Deep-Sea Res. Pt. 00, 49, 2017-2030.

Mélin, F., Hoepffner, N., 2004. 'Global marine primary production: A satellite view.' *JRC Publication*, EUR Report 21084EN, 211pp.

Mélin, F., Challis, J., Hoepffner, N., 2004. 'Photosynthetically Available Radiation : A practical approach for global applications.' *JRC Publication*, EUR Report 21016 EN, 60pp.

Mélin, F., Vantrepotte, V., 2007. Phytoplankton biomass and productivity in the Black Sea derived from the ocean colour record. Proceedings of the NATO Advanced Research Workshop on "Challenges for the Black Sea Operational Oceanography to Improve Regional Environmental Security", Balchik, Bulgaria, 25-27 sep. 2007, 15 pp.

Mélin, F., and Hoepffner, N., 2011. Monitoring phytoplankton productivity from satellite. In "Handbook of Satellite Remote Sensing Image Interpretation: Applications for Marine Living Resources Conservation and Management", EU PRESPO and IOCCG, Dartmouth, Canada, 293 pp., pp79-93.

McCarthy, J.J., Yilmaz, A., Coban-Yildiz, Y., Nevins, J.L., 2007. Nitrogen cycling in the offshore waters of the Black Sea. Estuar. Coast. Shelf Sci. 74, 493–514. http://dx.doi.org/10.1016/j.ecss.2007.05.005.

McQuatters-Gollop, A., L.D., Mee, D.E., Raitsos, and G.I., Shapiro, 2008: Non-linearities, regime shifts and recovery: the recent influence of climate on Black Sea chlorophyll. J. Mar. Syst. 74 (1), 649–658, https://doi.org/10.1016/j.jmarsys.2008.06.002

Mikaelyan, A. S., Shapiro, G. I., Chasovnikov, V. K., Wobus, F., and M. Zanacchi, 2017: Drivers of the autumn phytoplankton development in the open Black Sea, J. Mar. Syst., 174, 1 – 11, doi.org/10.1016/j.jmarsys.2017.05.006

Miladinova, S., A., Stips, E., Garcia-Gorriz, and D., Macias Moy, 2016: Modelling Toolbox 2: The Black Sea ecosystem model, EUR 28372 EN, doi:10.2788/677808

Miladinova, S., A., Stips, D., Macias Moy, and E., Garcia-Gorriz, 2017a: Revised Black Sea ecosystem model, EUR 28983EN, doi:10.2760/220233

Miladinova, S., A., Stips, E., Garcia-Gorriz, and D., Macias Moy, 2017b: Black Sea thermohaline properties: Long-term trends and variations, J. Geophys. Res., 122, 5624–5644, doi:10.1002/2016JC012644.

Miladinova, S., A., Stips, E., Garcia-Gorriz, and D., Macias Moy, 2018: Formation and changes of the Black Sea cold intermediate layer, Prog. Oceanogr., 167, 11-23, doi:10.1016/j.pocean.2018.07.002.

Miladinova, S., A., Stips, D., Macias Moy, and E., Garcia-Gorriz, 2020: Seasonal and Inter-Annual Variability of the Phytoplankton Dynamics in the Black Sea Inner Basin, Oceans, 1, 251-273, doi:10.3390/oceans1040018.

Moran, X.A.G., Estrada, M. 2005. Winter pelagic photosynthesis in the NW Mediterranean. Deep-Sea Res. Pt.I, 52,1806-1822

Moran, X.A.G., Taupier-Letage, I., Vazquez-Dominguez, E. Ruiz, S., Arin, L., Raimbault, P., Estrada, M. 2005. Physical-biological coupling in the Algerian Basin (SW Mediterranean): influence of mesoscale instabilities on the biomass and production of phytoplankton and bacterioplankton. Deep-Sea Res. Pt.I, 48, 405-437.

Moutin, T., Raimbault, P., 1996. Primary production, carbon export and nutrient availability in western and eastern Mediterranean Sea in early summer 1996 (MINOS cruise). J. Mar. Syst., 33, 273 – 288.

Murray J.W., Z. Top and E. Ozsoy (1991) Hydrographic properties and ventilation of the Black Sea. Deep-Sea Research, 38, S663-S689.

Neumann, T., 2000. Towards a 3d-ecosystem model of the Baltic Sea. J. Mar. Syst. 25, 405–419.

Nezlin, N.P., 2008: Seasonal and interannual variability of remotely sensed chlorophyll. The Handbook of Environmental Chemistry. Vol. 5, Part Q: The Black Sea Environment, Kostianoy, G., and A.N. Kosarev, Eds., Springer Verlag, 333–349.

Olesen, M., Lundsgaard, C., Andrushaitis, A., 1999. Influence of nutrients and mixing on the primary production and community respiration in the Gulf of Riga. J. Mar. Syst. 23, 127—143.

Oguz, T., H. Ducklow, P. Malanotte-Rizzoli, J.W. Murray, V.I. Vedernikov, and U. Unluata , 1999: A physical-biochemical model of plankton productivity and nitrogen cycling in the Black Sea. Deep-Sea Res. I. 46, 597–636.

Oguz, T., Ducklow, H.W., and Malanotte-Rizzoli, P., 2000: Modeling distinct vertical biogeochemical structure of the Black Sea: dynamical coupling of the oxic, suboxic and anoxic layers, Global Biogeochem. Cyc., 14, 1331–1352.

Oguz, T., Cokacar, T., Malanotte-Rizzoli, P., and Ducklow, H.W., 2003: Climatic warming and accompanying changes in the ecological regime of the Black Sea during 1990s. Global Biogeochem. Cycles, 17, 1088.

Oguz, T., Stips, A., Macias, D., Garcia-Gorriz, E. and Coughlan, C. 2014: Development of the Black Sea specific ecosystem model (BSSM), EUR27003EN, doi:10.2788/82470.

Pärn, O., Friedland, R., Garcia Gorriz, E. and Stips, A., Report on the biogeochemical model setup for the Baltic Sea and its applications, EUR 30252 EN, Publications Office of the European Union, Luxembourg, 2020, ISBN 978-92-76-19448-4, doi:10.2760/672255, JRC120378

Platt, T., Sathyendranath, S., 1988. Oceanic primary production: Estimation by remote sensing at local and regional scales. *Science,* 241, 1613-1620.

Psara, S., Tselepides, A., Ignatiades, L. 2000. Primary productivity in the oligotrophic Cretan Sea (NE Mediterranean): seasonal and interannual variability. Prog. Oceanogr. 46, 187 - 204

Purina, I., Labucis, A., Barda, I., Jurgensone, I., Aigars, J. 2018. Primary productivity in the Gulf of Riga (Baltic Sea) in relation to phytoplankton species and nutrient variability. Oceanologia, 60(4), 544-552.

Quay, P.D., Peacock, C., Bojrkman, K., Karl, D.M. 2010. Measuring primary production rates in the ocean: Enigmatic results between incubation and non-incubation methods at Station ALOHA. Global Biogeochemical Cycles, 24(3), doi: 10.1029/2009GB003665

Renk, H. 1993 Produkcja pierwotna Zatoki Puckiej. In Zatoka Pucka (Korzeniewski, K, ed.). Fundacja Rozwoju Uniwersytetu Gdan´ skiego, Gdan´ sk, pp. 338–365.

Richardson, A.J., Schoeman, D.S., 2004. Climate impact on plankton ecosystems in the Northeast Atlantic. Science 305, 1609–1612. https://doi.org/10.1126/science.1100958.

Saba, V.S., Friedrichs, M.A.M., Carr, M.-E., Antoine, A., Armstrong, R.A., Asanuma, I., Aumont, O., Behrenfeld, M.J., Bennington, V., Bopp, L., Bruggeman, J., Buitenhuis, E.T., Church, M.J., Ciotti, A.M., Doney, S.C., Dowell, M.D., Dunne, J., Dutkiewicz, S., Gregg, W.W., Hoepffner, N., Hyde, K.J.W., Ishizaka, J., Kameda, T., Karl, D.M., Lima, I., Lomas, M.W., Marra, J., McKinley, G.A., Mélin, F., Moore, J.K., Morel, A., O'Reilly, J., Salihoglu, B., Scardi, M., Smyth, T.J., Tang, S., Tjiputra, J., Uitz, J., Vichi, M., Waters, K., Westberry, T.K., Yool, A., 2010. The challenges of modeling depth integrated marine primary productivity over multiple decades: A case study at BATS and HOT. *Global Biogeochem. Cycles*, 24, GB3020, 10.1029/2009GB03655.

Saba, V.S., Friedrichs, M.A.M., Antoine, A., Armstrong, R.A., Asanuma, I., Behrenfeld, M.J., Ciotti, A.M., Dowell, M.D., Hoepffner, N., Hyde, K.J.W., Ishizaka, J., Kameda, T., Marra, J., Mélin, F., Morel, A., O'Reilly, J., Scardi, M., Smith, W.O., Smyth, T.J., Tang, S., Uitz, J., Waters, K., Westberry, T.K., 2011. An evaluation of ocean color model estimates of marine primary productivity in coastal and pelagic regions across the globe. *Biogeosciences*, 8, 489-503.

Skogen, M.D., Moll, A. 2001. Interannual variability of the North Sea primary production: comparison from two model studies. Cont. Self Res., 20, 129-151.

Steele, J.H., 1956. Plant production on the Fladen Ground. Journal of Marine Biology Association UK 35,1-33.

Stips, A., Dowell, M., Somma, F., Coughla, C., Piroddi, C., Bouraoui, F., Macias, D., Garcia-Gorriz, E., Cardoso, A.C., Bidoglio, G., 2015. Towards an Integrated Water Modelling Toolbox. European Commission, Luxemburg.

Stramska, M., Zuzewicz, A., 2013. Comparison of primary productivity estimates in the Baltic Sea based on the DESAMBEM algorithm with estimates based on other similar algorithms. Oceanologia, 55(1), 77-100, doi: 10.5697/oc.55-1.077

Sournia, A. 1973. La production primarie plactonique en Mediterranée; essai de mise á jour, contribution no. 81 of *Cybium*, Cooperative Investigations in the Mediterranean,.

Uitz, J., Stramski, D., Gentili, B., D'Ortenzio, F., Claustre, H. 2012. Estimates of phytoplankton class-specific and total primary production in the Mediterranean Sea from satellite ocean color observations. Global Biogeochemical Cycles, 26(2), doi: 10.1029/2011GB004055

Vedernikov, V.I. and A.B. Demidov, 1997: Vertical distributions of primary production and chlorophyll during different seasons in deep part of the Black Sea. Oceanology, 37, 376-384.

Volpe, G., Santoleri, R., Vellucci, V., d'Alcalà, M., Marullo, S., d'Ortenzio, F., 2007. The colour of the Mediterranean Sea: Global versus regional bio-optical algorithms evaluation and implication for satellite chlorophyll estimates. Remote Sens. Environ., 107, 625-638.

Wasmund**,** N**.**, Andrushaitis, N., Łsiak-Pastuszak, E., Muller-Karulis, B., Nausch, G., Neumann, T., Ojaveer, H., Olenina, I., Postel**, L.,** Witek**,** Z. 2001. Trophic Status of the South-Eastern Baltic Sea: A Comparison of Coastal and Open Areas. Estuarine, Coastal and Shelf Science, 56

Weston, K., Fernand, L., Mills, D.K., Delahunty, R., Brown, J., 2005. Primary production in the deep chlorophyll maximum of the central North Sea. J. Plank. Res., 27(9), 909-922.

Yunev,O.A.,2011.Eutrophication and anual primary production of phytoplankton in the deep-water part of the Black Sea.Oceanology 51, 616–625.

Yunev, O.A., Vedernikov, V.I., Basturk, O., Yilmaz, A., Kideys, A.E., Moncheva, S., Konovalov, S.K., 2002. Long-term variations of surface chlorophyll a and primary production in the open Black Sea. Mar. Ecol. Prog. Ser. 230, 11–28. http://dx.doi.org/10.3354/meps230011.

Zervoudaki, S., Nielsen, T., Christou, E., Siokou-Frangou, I. 2006. Zooplankton distribution and diversity in a frontal area of the Aegean Sea. Mar. Biol. Res., 2, 149 – 168.

GETTING IN TOUCH WITH THE EU

In person

All over the European Union there are hundreds of Europe Direct information centres. You can find the address of the centre nearest you at: https://europa.eu/european-union/contact_en

On the phone or by email

Europe Direct is a service that answers your questions about the European Union. You can contact this service:

- by freephone: 00 800 6 7 8 9 10 11 (certain operators may charge for these calls),

- at the following standard number: +32 22999696, or

- by electronic mail via: https://europa.eu/european-union/contact_en

FINDING INFORMATION ABOUT THE EU

Online

Information about the European Union in all the official languages of the EU is available on the Europa website at: https://europa.eu/european-union/index_en

EU publications

You can download or order free and priced EU publications from EU Bookshop at: https://publications.europa.eu/en/publications. Multiple copies of free publications may be obtained by contacting Europe Direct or your local information centre (see https://europa.eu/european-union/contact_en).

KJ-NA-30546-EN-N

The European Commission's science and knowledge service

Joint Research Centre

JRC Mission

As the science and knowledge service of the European Commission, the Joint Research Centre's mission is to support EU policies with independent evidence throughout the whole policy cycle.

EU Science Hub

ec.europa.eu/jrc

@EU_ScienceHub

EU Science Hub - Joint Research Centre

EU Science, Research and Innovation

EU Science Hub

Publications Office of the European Union

doi:10.2760/19851

ISBN: 978-92-76-27860-3